Subject-specific three-dimensional finite element model of the human knee complex

Submitted by Kulchamai Thienkarochanakul to the University of Exeter

as a thesis for the degree of

Doctor of Philosophy in Engineering

In August 2018

I certify that all material in this thesis which is not my own work has been identified and that no material has previously been submitted and approved for the award of a degree by this or any other University.

Signature: ……

Abstract

Knee Osteoarthritis (OA) is a common medical condition that necessitates primary care for 1 in 5 adults over the age of 45 only in the UK. This causes functional limitations and decreases the quality of life. The OA is a metabolically active process which involves all joint tissues, i.e. bone, synovium and muscle which causes some symptoms such as persistent knee pain, morning stiffness and reduced functional capabilities. Most of the disability observed in knee OA is mainly because of pain. This mechanism is usually intensified by daily activities and the pain can relax by rest. Therefore, clinicians are interested to analyse this vital component, while accessing the internal structures such as cartilage or the menisci which is impossible *in-vivo*. Therefore, computational image-based models are effective tools in order to analyse the biomechanical causes of the OA. In this study, a three-dimensional finite element (FE) model of a healthy knee was constructed, using scanned MRI data. Bones, articular cartilages, menisci, patella, patella tendon and all the relevant ligaments were included in the model in their bio-realistic structures. 3D gait measurements were analysed to define loading and boundary conditions. After validation, the 3D finite element model was used to analyse the possibility of osteoarthritis condition and degeneration within the menisci and knee cartilage tissues. It was shown that the medial region of cartilage layers and menisci in the knee joint sustain higher values of stress for the OA conditions, while for the healthy knee, the stresses are more evenly distributed across the cartilage. This suggests that any treatment for knee osteoarthritis should focus more on the medial region of the tibiofemoral cartilage. Furthermore, the analysis of varus condition was added to the developed OA model and the results showed that the varus condition can exacerbate the OA.

Table of Contents

Total word count: 22,244 words

List of Figures

List of Tables

Acknowledgement

I would like to thank my research advisor, Professor A.A. Javadi, for spending numerous hours on tedious editing for days (and nights) on end to help transform my soulless prattling into thoughtful and engaged writing. Without his exceptional patience in responding to painfully similar and repetitive questions.

Thank you, Professor Philippe Youngs, for introducing and supporting with the software that was used within this research.

Special thanks to Dr. Mohammad Akrami for assisting and guiding me through the process of creating the three-dimensional finite element model.

Special thank you to Dr. Abdelmalek Benattayallah from Medical school for assisting and providing the knowledge of the MRI scanner.

Finally, I would like to thank my family and friends for the greatest support, advising, consulting and cheering through all the tough and good times.

Hopefully, by the time this is finalized, I will have found gainful employment and, in doing so, justified the investment of your time and effort. You are very good to me.

Abbreviation

2D	Two Dimension
3D	Three Dimension
ACL	Anterior Cruciate Ligament
BW	Body weight
CAD	Computer Aided Design
CPU	Central Processing Unit
CT	Computed Tomography
DOF	Degree of Freedom
DICOM	Digital Imaging and Communication in Medicine
E	Young’s Modulus
F	Force
FE	Finite Element
FEA	Finite Element Analysis
FEM	Finite Element Method
G	Shear Modulus
GCS	Global Coordinate System
GRF	Ground Reaction Force

HKA	Hip Knee Ankle
JCS	Joint Co-ordinate System
Kg	Kilogram
KOA	Knee Osteoarthritis
LBA	Load Bearing Axis
LCL	Lateral Collateral Ligament
MCL	Medial Collateral Ligament
MEMs	Micro electromechanical systems
MRI	Magnetic Resonance Imaging
N	Newton
OA	Osteoarthritis
PCL	Posterior Cruciate Ligament
PRS	Plate Reference System
v	Poisson’s Ratio

1. Introduction

1.1. Background

Knee osteoarthritis (OA) is one of the most common form of arthritis, especially in middle-aged people and seniors, affecting very large number of people worldwide (Arthritis Research UK, 2013). It is a degenerative joint disease that causes wear and tear in the cartilage surface, causing pain as well as swelling and loss of joint mobility. The key role of cartilage in the knee joint is to contribute to knee movement and to absorb the shocks during movement (Arthritis Research UK, 2013), so it is clear that knee OA can lead to debilitating life effects.

OA is accompanied by pain and can lead to constraints related to mobility, long-term disability and increased morbidity. OA causes damage to the joints and the tissue within and around the joint will show mild swelling. Knee OA can occur due to many causes, i.e. rheumatoid, ligament deterioration, sport injuries, etc., causing degradation of knee ligaments and muscle, or deflection of cartilage tissues that are in between the femur and tibia (Coleman and Roubenoff, 2012). The cartilage between the bones gradually wears away, causing a painful sensation as bones rub on one another. Menisci are rubbery pads that sits between the upper and lower leg bones (Arthritis Research UK, 2013), and these also degrade during the course of the disease, worsening its effects and causing pain within the joint, as cartilage and meniscus do not regenerate itself.

There has been significant amount of research focusing on determining the varus and valgus condition by changing the angles of the knee joint (Bendjaballah, Shirazi-Adl and Zukor, 1997; Gardiner and Weiss, 2006; Hopkins *et al.*, 2010;

Yang *et al.*, 2010; Tarniţă, Catana and Tarnita, 2014; Sun *et al.*, 2016). There are two main difficulties in this research; first, models extracted from Magnetic Resonance Imaging (MRI) are unable to indicate anatomy axes accurately due to the sample size of the human knee joint. Second, due to the uncertainty as to where the anatomical axes are located, changes in angle cannot be properly performed. There is a high chance that change in angle will be identified incorrectly. Further, when there are validated models of a healthy knee, it is not worth the attempt to create a varus-valgus angle without identifying the right location of the anatomy axis and mechanical axis. These are the reasons why there are very few research studies which use FE models to work on varus-valgus. Due to lack of data in the existing literature, therefore, the link between movement quality and risk of injury remains unclear. However, in this study, the experiment will be focusing on engineering static parameters, moment, and if these parameters could be applied to the model, then the problem of uncertainty of the location of the moment axis would be solved.

1.2. Anatomy of a Knee Joint

The knee is the largest and most complicated joint in the human body. It is also the most vulnerable because it bears enormous weight and pressure loads (Ethier and Simmons, 2008). The knee joint is made up of three bones (hard tissues) and a variety of soft tissues. The four bones are the femur, the tibia, the fibula, and patella (Ethier and Simmons, 2008) (see Figure 1-1).

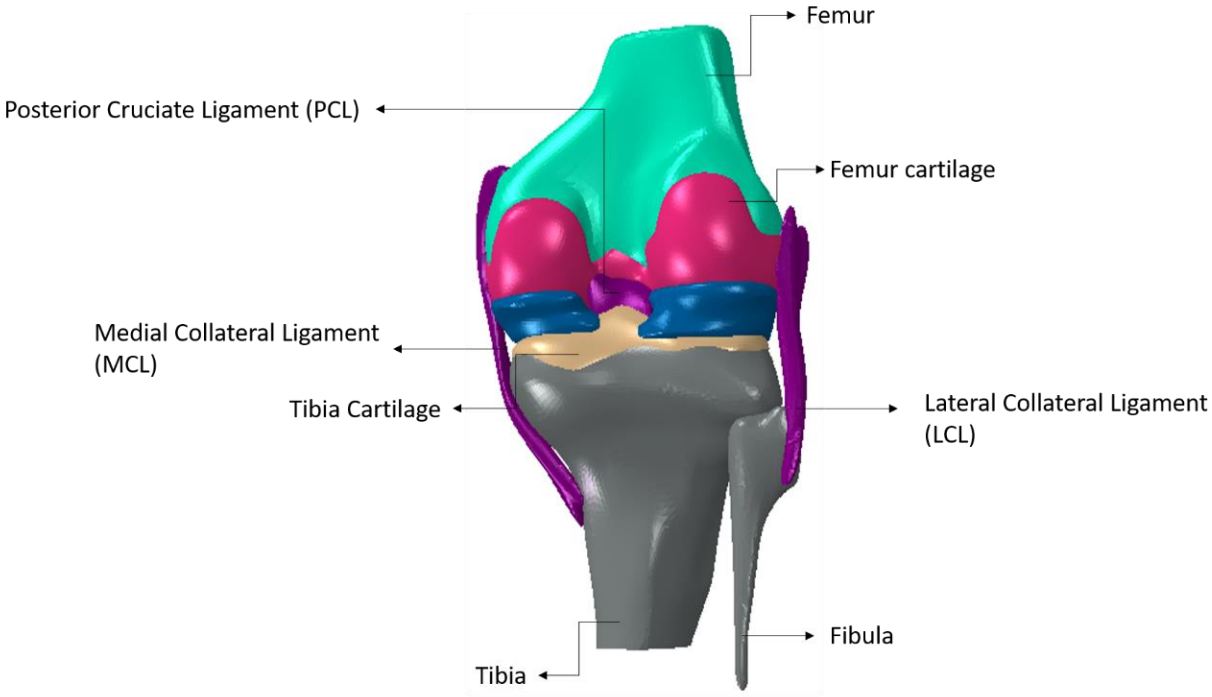

Figure 1-1 Composition of the human knee joint

The articulating ends of the femur and tibia are divided into two condyles. The femoral condyles are round and bulbous, with a slight gap between the two. The tibial condyles have a slight indentation to accommodate the femoral condyles, with a slight ridge dividing them. Each has a layer of articular cartilage covering its articulating surfaces. In the gap between femoral and tibial cartilage, a pair of menisci wraps around the condyles. These are all surrounded by a fluid-filled capsule, ensuring that the soft tissues are saturated with synovial fluid (Ethier and Simmons, 2008).

1.2.1. Bones

The femur, tibia, fibula and patella are the four bones that create a knee joint, and are covered by articular cartilage in their distal, proximal and anterior ends. The femur is the largest, longest and heaviest bone in the human body; it is the main

structural element of the knee joint (Marieb *et al.*, 2013; Hall, 2015; Tortora and Derrickson, 2018).

The distal end of femur expands into the large medial and lateral condyles that constitute the proximal articular surface of the knee joint (Levangie and Norkin, 2011a; Tortora and Derrickson, 2018). The tibia is second largest bone in the the knee joint after the femur. It supports the weight of the body from the femur and transmits it to the foot.

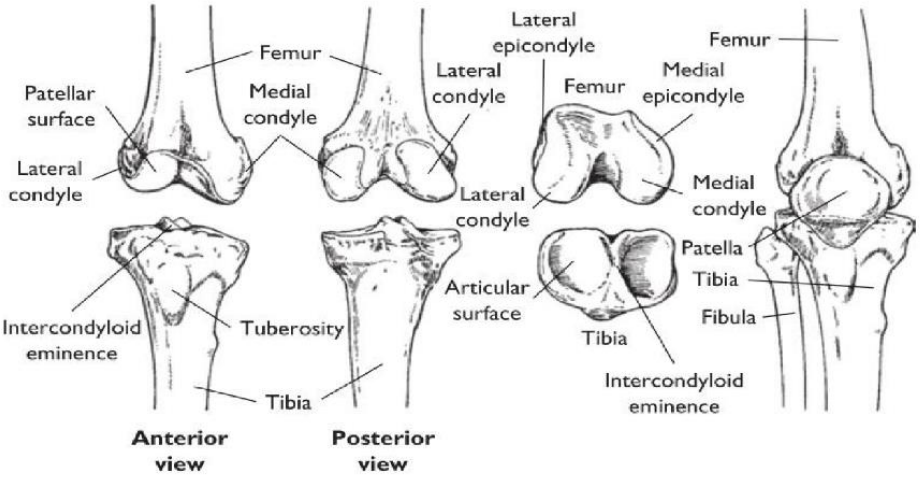

Figure 1-2 Bony structure of the knee (Hall, 2015)

As shown in Figure 1-2, at the proximal end of the tibia is asymmetrical and concave (Marieb *et al.*, 2013). Medial and lateral condyles (or tibial plateaus) constitute the distal end of the knee joint (Levangie and Norkin, 2011a). The tibial condyles articulate with the corresponding condyles of the femur (Marieb *et al.*, 2013) which are separated by intercondylar tubercles, two bony spines, and a roughened area. During knee extension, these tubercles lodge in the intercondylar notch of the femur (Levangie and Norkin, 2011a). Distally, the tibia

has a concave shape and articulates with the talus bone of the foot (Marieb *et al.*, 2013; Hall, 2015).

1.2.2. Articular Cartilage

The bones at a synovial joint, such as the knee, are covered by articular cartilage, which is hyaline cartilage (Tortora and Derrickson, 2018). In the knee, articular cartilage is present at the end of the femur, the top of the tibia and the posterior side of the patella (Darrow, 2001).

Cartilage is a firm and strong tissue which covers the bone ends, and it also forms some other body parts, such as nose, ears, and etc. (Jin, 2014). Its structure is primarily assumed to be a fibre matrix, but in some cases is considered a fibre-reinforced composite material.

Articular cartilage is a soft, porous, and permeable tissue that is hydrated. It consists of specialised cells called chondrocytes embedded in an extracellular matrix (ECM) of collagen fibres, proteoglycans, and non-collagenous proteins (Levangie and Norkin, 2011a). Articular cartilage can be divided into three different layers or zones with different collagen fibre orientations and, consequently, with different roles in shock absorption and friction reduction. There is a fourth layer, the calcified layer of cartilage that lies adjacent to subchondral bone and anchors the cartilage securely to the bone. Unfortunately, once injured, hyaline articular cartilage has only limited and imperfect mechanisms for self-repair (Levangie and Norkin, 2011b). Therefore, injuries to this tissue tend to regress, deteriorating more and more the protective coating of the bone ends, leading to the development of knee OA (Hall, 2015).

1.2.3. Menisci

Since the bony structure of the tibial plateaus does not match up well with the convexity of the femoral condyles, an intermediary is necessary, to mediate this complexity of the two bone structures; this role belongs to the menisci, which are two semi-circular discs of fibrocartilage, lying within the tibiofemoral joint and covering one half to two-thirds of the articular surface of the tibial plateau (Levangie and Norkin, 2011b)(see Figure 1-3).

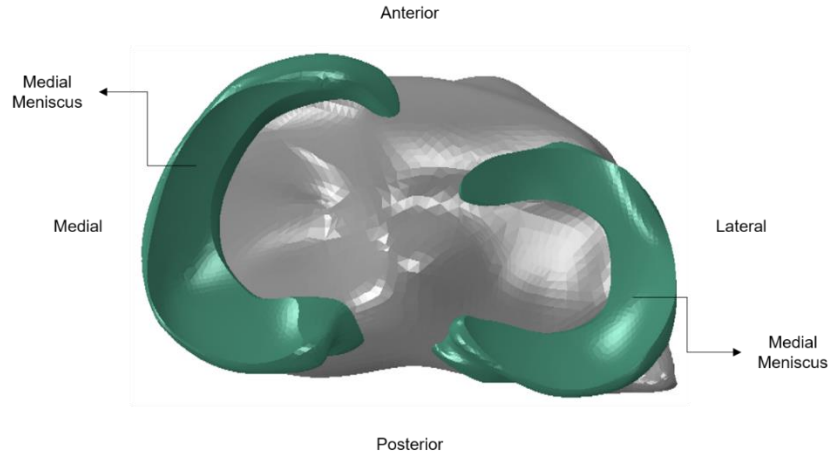

Figure 1-3 Superior view of the right tibia in the knee joint, highlighting the menisci

The menisci perform several essential roles in joint mechanics and function. One major role is to transmit loads and reduce pressure on articular cartilage. Another is lubrication and distribution of synovial fluids whereas the cartilage protects bones from rubbing on one another (Ethier and Simmons, 2008).

The medial meniscus is directly attached to the medial collateral ligament (MCL) (Hall, 2015). The menisci help prevent side-to-side rocking of the femur on the tibia (Marieb *et al.*, 2013); they also enhance joint congruence (Levangie and Norkin, 2011b), assist with load transmission (Hall, 2015) and act as shock absorbers (Marieb *et al.*, 2013).

1.2.4. Ligaments

The femur and the tibia are connected by four major ligaments, the anterior cruciate ligament (ACL), the posterior cruciate ligament (PCL), the medial collateral ligament (MCL), and the lateral collateral ligament (LCL). The anterior and posterior cruciate ligaments pass through the gap between the two femoral condyles (see Figure 1-1). The lateral and medial collateral ligaments attach to the outsides of the lateral and medial condyles respectively. These ligaments both ensure that the femur and tibia remain in contact and control the relative positioning of these two bones during knee flexion (Ethier and Simmons, 2008). Water is the main reason for the nonlinear viscoelastic behaviour of ligaments With increased age, ligament tissue becomes more mature, and this vastly influences its properties, e.g. collagen fibres increase in size, molecular cross-links increase in number and tissues dry out (Nigg and Herzog, 2007).

1.3. Varus and valgus

The technical terms of ‘varus’ and ‘valgus’ knee are generally known as bowed leg knee and knocked knee (Kamath *et al.*, 2010). Varus and valgus are a limb deformation which occurs in joints due to several diseases such as osteoarthritis (OA).

To get a comprehensive understanding of varus and valgus conditions, it is important to understand knee structure and its alignment. In general, a healthy knee joint is 181° aligned with the femur head and the centre of the ankle as shown in Figure 1-4. The most important axis is the mechanical axis that aligns the joint.

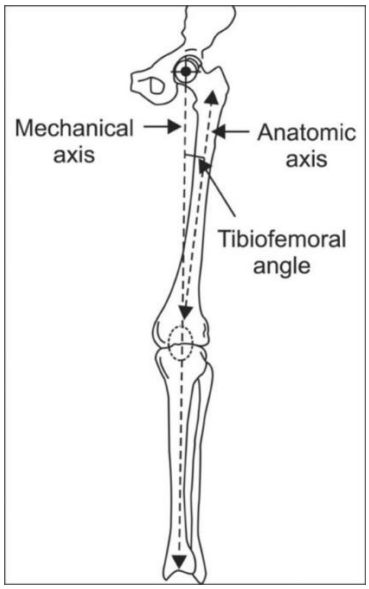

Figure 1-4 Alignment of the lower extremity of the human body (Donaldson, Joyner and Tudor, 2015)**.**

Misalignment of the mechanical axis, or also known as load bearing axis (LBA), is the main cause of varus and valgus deformation. Figure 1-5 shows the differences between varus and valgus compared to a normal knee joint. Figure 1-5 (A) describes varus as a bowed leg, where the medial region has been affected by the disease and the lateral region has lifted forming a bowed leg. Valgus is the opposite of varus (Figure 1-5 C), the lateral region is affected by the disease while the medial region has lifted forming a knocked knee.

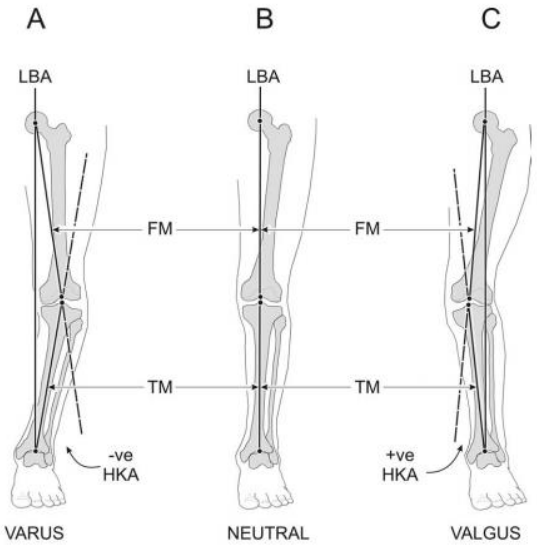

Figure 1-5 Common frontal plane lower limb alignment patterns. (A) Varus alignment: knee centre is lateral to the LBA (HKA is negative). (B) Neutral alignment: knee centre is located on the LBA (HKA = 0°); femoral and tibial mechanical axes are colinear. (C) Valgus alignment: knee centre is medial to the LBA (HKA is positive). LBA: load-bearing axis, HKA: hip-knee-ankle angle, FM: femoral mechanical axis, TM: tibial mechanical axis (Derek *et al.*, 2007)**.**

1.4. Aims and Objective

The aim of this thesis is to clarify a finite element model of osteoarthritis and to use a different approaches of loading by using moment within finite elements to replicate the varus and valgus deformation instead of changing the initial angle of the model during assembly.

The main objectives of this study are:

- to summarise available data, previous test methods, and the moment that is used in the knee joint.

- to set up a specific test of moment on the knee in varus by using finite element analysis. This will be done by:

i. Constructing a detailed human knee structure which consists of the bones, cartilages, and encapsulated soft tissue which host all the other segments based on their anatomical structures shown in the medical image processing software, ScanIP, and the Computer Assisted Design (CAD) software SOLIDWORKS.

ii. Using simulated results and predictions to conduct an extensive parametric study and sensitivity study.

iii. Analysing the stress within the OA knee joint using a variety of approaches gathered from the literature.

1.5. Thesis Outline

In accordance with the objectives mentioned above, this thesis is divided into 7 chapters and is followed by references.

Chapter 2 reviews the literature concerning biomechanical research involving the human knee joint, covering research related to normal knee function, knee joint moment, gait behaviour, knee modelling and testing, as well as finite element (FE) simulation of knee joints and other parts of the leg.

Chapter 3 explains the details of modelling and segmentation based on Bio-CAD image-based technique. This chapter also presents the collection and processing of data on the variation of varus angles of the human knee joints and variations in ground reaction forces while the subject performs various tests, such as walking on a set of force platforms.

Chapter 4 is dedicated to construction of the finite element model construction of the knee complex showing how the parts are assembled to configure healthy knee. Material properties, contacts, meshing different knee segments, loads, and boundary conditions are assigned to the healthy model. Before the analysis stage, this process is repeated with different parameters and simulations with different material properties for OA knees, and to replicate the varus angle by using moment for varus knee. The model is then validated against data drawn from the literature, and the validation process is explained in detail.

In Chapter 5, the results of finite element simulations on osteoarthritis using commercial software, ABAQUS, are presented. This chapter shows the differences between a healthy knee and an OA knee for the purpose of verification regarding results from the literatures. In order to accomplish this, it is necessary to obtain and analyse distribution maps and the maximum values of the von Mises stresses and displacements.

In chapter 6, the model is used to predict the biomechanical behaviour of the knee bones, ligaments, cartilage and menisci for different gait phases in order to analyse how parameters such as stress has changed with the material properties and the modification of the model. These extracted results can later be compared against predictions from the current computational models or against data from the available experimental literatures.

The thesis ends with discussion in Chapter 7 of valuation of the results of the research carried out for this thesis as well as discussion of future research directions.

2. Literature Review

2.1. Introduction

The human knee is a complex structure, having roles in providing structure, absorbing shocks, and facilitating the gait pattern. Analysing this vital joint can provide valuable knowledge of its structure and functions. As accessing the internal structure of the human body is not possible *in-vivo*, computational techniques such as the finite element method have been widely used to investigate the functional roles of the knee (Rayfield, 2007). Several studies have been conducted by developing 2D or 3D models. In this chapter, the details of knee anatomy are presented, before the main outcomes of published studies about the biomechanics of the knee joint are discussed. Although some researchers have used 3D finite element models, such studies related directly to the evaluation of knee joint moment are rare. Therefore, almost all details of rotation of the knee joint included in this literature review are drawn from other methodologies, other mathematical models, or other computational models rather than from finite element models.

The objectives of this research are to create and to validate a general-purpose numerical knee joint model and to use the finite element method to evaluate and to demonstrate the results. This will involve using a human CT (Computer Tomography) or MRI (Magnetic Resonance Imaging) scan to provide an accurate geometry, from which a finite element model will be created. This thesis focuses specifically on the material model of the knee's components. In other words, it aims to develop a large-scale subject-specific human knee model in three

dimensions to be used to analyse biomechanical applications. This first, subject specific model will serve as a base model upon which more advanced models can be built. Various loadings will be applied to both healthy and OA knee models, in order to evaluate performance differences and to compare these with the results of previous research studies.

This study will use experimental and numerical methods to identify the stress occurring during midstance or standing. The finite element analysis (FEA) software ABAQUS software (ABAQUS Inc., USA) will be used to identify the contact areas and the effects of stress on the meniscus and tibial and femoral cartilage during midstance based on the extracted force from the experimental data. Moreover, the FE model will be used to analyse the variations in contact pressure and stress distributions of the main deformable knee components.

2.2. Knee OA and Knee Joint Injuries

There are many different types of arthritis, such as rheumatoid arthritis and gout, that cause a wide range of symptoms; one of the most common is osteoarthritis (OA). OA affects joints or cartilage, and patients who have OA will feel pain and stiffness. Cartilage allows bones to glide over each other and helps to absorb the shock from the bones. In OA, the cartilage is worn away and broken down which causes the bones under the cartilage to rub together. This causes pain, stiffness and a grating or grinding sensation (crepitus) when the joint moves, resulting in swelling (either hard or soft) and restricted movement in the affected joint. This may cause a great deal of difficulty in daily life activities such as climbing the stairs. An OA knee can appear as either varus or valgus knee, and noise in the joint with pain. Knee OA is a degenerative disease that will cause crippling if left untreated. Regrettably, in old age, everyone will develop knee OA to some extent (Siegel, Vandenakker-Albanese and Siegel, 2012).

In general, people near the age of 45 often have inflammatory arthritis such as rheumatoid arthritis, post-traumatic arthritis, septic arthritis, or reactive arthritis. Degenerative OA is often caused by the meniscus damage, cartilage degeneration, ligament elongation, or paralysis. (Arthritis Research UK, 2013). Figure 2-1 shows a human knee joint that has been deformed by OA.

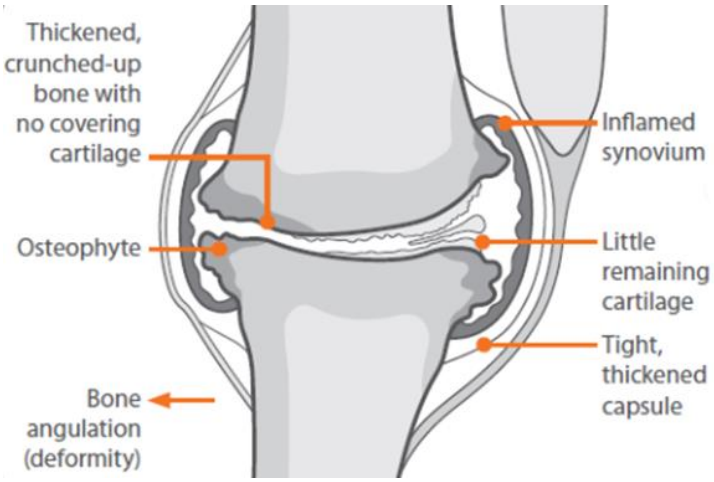

Figure 2-1 A human knee joint that has been deformed by severe OA (Arthritis Research UK, 2013)

2.3. Mechanical Functions and modelling of the Knee Joint

All joints in the body move through varying degrees of movement in all three planes of motion (sagittal, frontal, transverse) at once (Figure 2-2).

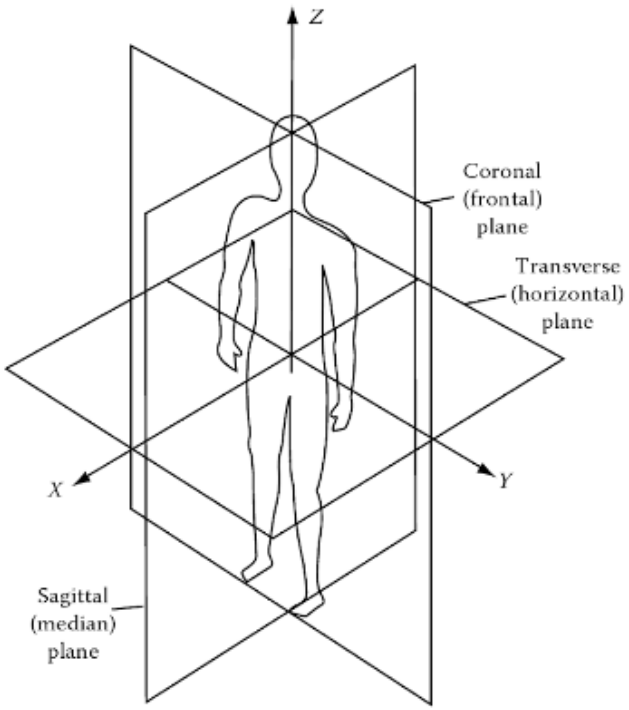

Figure 2-2 Anatomical plane (Huston 2008)

2.3.1. Moments

Varus and valgus is a condition that form with knee OA, with the understanding of the alignment of the human lower extremity (see Figure 1-4). Human body weight is transferring from one joint to another in a straight line following the mechincal axis, with varus or valgus condition, human weight has shifted with slight angle according to how extreme is the varus or valgus condition. The shape of the menisci increases the contact area between the femur and the tibia, contributing to the reduction of the joint stress on the articular cartilage of the knee (Hall, 2015). It is estimated that the menisci take up 50% to 70% of the compressive forces that are applied to the knee in activities such as normal walking, stair climbing (one to two times the body weight) and running (three to four times the body weight) (Levangie and Norkin, 2011a). This function is depicted in Figure 2-3.

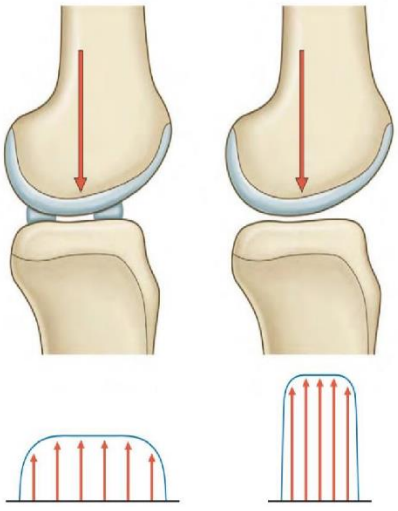

Figure 2-3 The menisci play a major role in increasing tibiofemoral congruence. The wedge-shaped cross-section of the menisci helps to increase the contact area between the femur and the tibia, leading to a wider distribution of compressive loads (Standring and Borley, 2008)

In meniscus-deficient knees, the stresses at the tibiofemoral joint can be up to three times higher than in a healthy knee. So, as with injury to the articular cartilage, an injury to the menisci, increases the wear on the articulating surfaces, leading to a knee joint more susceptible to the development of degenerative conditions (Hall, 2015).

2.4. Material Properties

The complexity of the human knee FE model in addition to its high integration of various material types leads researchers to simplify the material properties in their research models. The most significant material properties for building an FE model and in particular for studying hard tissues are Young's modulus and the Poisson's ratio. Young's modulus or modulus of elasticity (E) describes the elastic tendency of the material to deform, under axial loading conditions. Mathematically, the value of Young's modulus is given by the slope of the linear part of the stress-strain curve of a material. The Poisson's ratio (v) is the ratio of the lateral or transverse strain to the axial or longitudinal strain.

2.4.1. Material Properties of Human Bones

A wide range of values has been reported in the literature for Young's modulus of bone, from 400 MPa (Donahue, Hull and Rashid, 2002; John, Pinisetty and Gupta, 2013; Kiapour *et al.*, 2014) to 20 GPa (Wang, Fan and Zhang, 2014). In some cases, the bones are assumed to be rigid and therefore no values are used for the material properties of the bony segments (Bendjaballah, Shirazi-Adl and Zukor, 1995, 1997; Limbert, Taylor and Middleton, 2004; Peña, Calvo, *et al.*,

2005; Peña *et al.*, 2006). Bones in the human skeletal system can be categorised as “cortical” and “trabecular or cancellous” based on their microstructure and porosity (Jin, 2014). In some FE studies of the human knee, in order to have more detailed material properties, the cortical and trabecular bone structures were distinguished by assigning different values to each (Donahue, Hull and Rashid, 2002; Cartana et al, 2013; Kiapour *et al.*, 2014). This is based on the fact that cortical bones can sustain higher stresses and bear more weight than cancellous bones (Akrami *et al.*, 2018) whereas cancellous bony structures can store more energy due to their larger surface areas (Hayes and Mockros, 1971) (see

).

Table 2-1 Summary of material properties of human bones

Reference	*Young's Modulus (MPa)*	*Poisson's ratio (v)*	*Element type*	*No. of Element*
(Donahue, Hull and Rashid, 2002)	400	0.3	8-nodes trilinear hexahedral	6000
(Peña, Calvo, et al.*, 2005)*	N/A	N/A	4-node surface	4783
(Peña et al.*, 2006)*	N/A	N/A	4-node surface	4783
(Cartana et al, 2013)	Cortical Femur 18,600 Cortical Tibia 12,500 Spongio bone 500	0.3	Elastic	N/A
(Kiapour et al.*, 2014)*	Trabecular bone 400	0.3	Hexahedral	N/A
(Wang, Fan and Zhang, 2014)	20,000	0.3	Hexahedral	N/A

Reference	*Young's Modulus (MPa)*		*Poisson's ratio (v)*	*Element type*	*No. of Element*
(Sun et al.*, 2016)*	Femur	17,000	0.3	Tetrahedral	N/A
	Tibia	12,200	0.3		
	Fibula	15,500	0.24		

2.4.2. Summary of Material Properties of Articular Cartilage

The literature shows that the elastic modulus of articular cartilage is in the range of 5 to 12 MPa and the Poisson's ratio in the range of 0.45 to 0.475. In the early years, Bendjaballah, Shirazi-Adl and Zukor, (1995 and 1997) assumed that the material properties of the articular cartilage were an isotropic, giving it an elastic modulus of 12 MPa and a Poisson's ratio of 0.45. Researchers such as Cartana et al (2013) used the same material properties but Poisson's ratios different from those used by Bendjaballah, Shirazi-Adl and Zukor, (1995 and 1997); they have set the E at 12 MPa and used v at 0.475. Donahue, Hull and Rashid (2002) and Kiapour *et al.* (2014) have used the same Poisson's ration as Cartana et al (2013).

Likewise, researcher have chosen varying value for the Young's modulus of articular cartilage. For example, Kiapour *et al.* (2014) have set the material elastic modulus of 15 MPa. Still other researchers, such as Peña, Martínez, *et al.*, (2005), Peña *et al.*, (2006) and Sun *et al.*, (2016) have used the material property of 5 MPa with the Poisson's ratio of 0.46. There is also research done by Wang, Fan and Zhang (2014), which has compared the stress results on the knee cartilage. The analysis was done using a wide range of Poisson's ratio from 0.05 to 0.46 with the material property of 10 MPa.

summarized the various numbers for the material properties of human articular cartilage that have been used in the literature.

Table 2-2 Summary of Material properties of articular cartilage

Reference	Young's Modulus (MPa)	Poisson's ratio (v)	Element type	No. of Element	Note
(Bendjaballah, Shirazi-Adl and Zukor, 1995)	12	0.45	8-node solid	374	
(Bendjaballah, Shirazi-Adl and Zukor, 1997)	12	0.45	8-node solid	374	
(Donahue, Hull and Rashid, 2002)	15	0.475	8-nodes trilinear hexahedral	5500	
(Peña, Calvo, *et al.*, 2005)	5	0.46	8-node brick	5195	No. of elements includes cartilages, meniscus and ligaments
(Peña *et al.*, 2006)	5	0.46	8-node brick	5195	No. of elements includes cartilages, meniscus and ligaments
(Cartana et al, 2013)	12	0.475	Elastic	N/A	
(Kiapour *et al.*, 2014)	15	0.475	Elastic	N/A	Hexahedral

Reference	Young's Modulus (MPa)	Poisson's ratio (v)	Element type	No. of Element	Note
(Wang, Fan and Zhang, 2014)	10	0.05-0.45	Elastic	N/A	Hexahedral
(Sun *et al.*, 2016)	5	0.46	Elastic	N/A	Tetrahedral

2.4.3. Summary of Material Properties of the meniscus

In a healthy knee joint, the medial and lateral menisci are crescent-shaped cushion that sits between the femur and tibia. (Giorgiafiorio, 2018).

Error! Reference source not found. shows the detail of the material properties that have been used for the meniscus in the literature.

Table 2-3 Summary of Material properties of the meniscus

Reference	Young's Modulus (MPa)		Poisson's ratio (v)		Element type	No. of Element	Note
(Bendjaballah, Shirazi-Adl and Zukor, 1995)	8		0.45		Hypoelastic	1212	
(Bendjaballah, Shirazi-Adl and Zukor, 1997)	8		0.45		Hypoelastic	1212	
(Donahue, Hull and Rashid, 2002)	Axial/radial Circumference	20 140	In Plane Out of plane	0.2 0.3	8-nodes trilinear hexahedral	2500	Stiffness: 2000 N/mm
(Peña, Calvo, *et al.*, 2005)	59		0.49		8-node brick	5195	No. of elements includes cartilages, meniscus and ligaments

Reference	Young's Modulus (MPa)		Poisson's ratio (v)		Element type	No. of Element	Note
(Peña *et al.*, 2006)	59		0.49		8-node brick	5195	No. of elements includes cartilages, meniscus and ligaments
(Cartana et al, 2013)	59		0.49		Elastic	N/A	
(Wang, Fan and Zhang, 2014)	Axial/ radial	20	In plane	0.2	Elastic	N/A	Hexahedral
	Circumference	140	Out of plane	0.3			
(Sun *et al.*, 2016)	59		0.49		Elastic	N/A	Tetrahedral

2.4.4. Summary of Material Properties of Ligaments

Ligaments are another important structure that supports the stability functioning of the knee joint. The four major ligaments of the knee joint are the medial collateral ligament (MCL), the lateral collateral ligament (LCL), the anterior cruciate ligament (ACL) and the posterior cruciate ligament (PCL) (Standring and Borley, 2008; Giorgiafiorio, 2018). These ligamentous structures connect the knee joint by attaching on the bones. Ligaments play a key role in providing passive stability to the joint throughout its full range of motion.

A full understanding of the role of each individual ligament in the restraining of motion is essential both for the development of an adequate diagnostic model and for determination of the proper surgical procedures in the specific case (Blankevoort *et al.*, 1991; Peña *et al.*, 2006). Hence, it is important to properly model and predict the mechanical behaviour of these biological tissues as this will yield information that would be difficult or impossible to obtain empirically.

The material properties of the different ligaments have been determined using optimisation between cadaver experiments and numerical simulations (see Table 2-4).

Table 2-4 Summary of Material properties of ligaments

Reference	Young's Modulus (MPa)	Poisson's ratio (v)	Element type	No. of Element	Note
(Donahue, Hull and Rashid, 2002)	Axial/radial 20 Circumference 140	In Plane 0.2 Out of plane 0.3	8-nodes trilinear hexahedral	2500	Stiffness: 2000 N/mm
(Peña, Calvo, *et al.*, 2005)	Hyperelastic	Hyperelastic	8-node brick	5195	No. of elements includes cartilages, meniscus and ligaments
(Peña *et al.*, 2006)	Hyperelastic	Hyperelastic	8-node brick	5195	No. of elements includes cartilages, meniscus and ligaments
(Cartana et al, 2013)	10	0.49	Elastic	N/A	
(Sun *et al.*, 2016)	6	0.4	Elastic	N/A	Tetrahedral

2.5. Objectives, Assumptions, Methods, Loading, and Boundary Conditions

Various types of assumptions have been made in the previous studies of knee joint FE analyses based on the specific research objectives (see Table 2-5). In many cases, biomechanical engineers and researchers working on subject-specific projects have created their own models; such models cannot be used by other researchers as prototypes. This is because of the limitations of different purposes, availability of equipment used, cost, and time factors, which are rarely stated in research papers. It is also difficult to directly compare results from one study to another due to the differences in model construction, and the material properties, contacts, and boundary conditions that are assigned. The model used in one study may be too complex or too simple for other projects with different purposes. Within particular line of knee joint studies, there are various modelling approaches according to subject-specific projects as stated in Table 2-5 Objectives, methods, structures and simulation of human knee FEA model. Another limitation in this area of research and modelling lies in how a 3D model may be created from a set of MR images. Due to the quality of the images, it is not possible to segment the muscles around the knee joint from the MR image to differentiate one from the other. Also, as the model that was segmented in this thesis does not contain muscles, it is unable to simulate muscle force.

In order to study the knee joint and related parts, different studies have considered different aims and objectives depending on the focus of the study. For example, some projects studied gait behaviour (Cartana et al, 2013) while some investigated knee pain and knee part deficiency, e.g. ACL deficiency, meniscal

damage, meniscal extrusion, malalignment, and joint laxity to subsequent cartilage loss (Limbert, Taylor and Middleton, 2004; Fernandes, 2014); others have worked on the kinematics of musculoskeletal components of the knee joint, and so on. Most of these research studies have developed models for their specific purposes, depending on equipment and subject-specific designs. The models have been designed in either two or three dimensions depending on the research objectives.

Modelling a detailed knee joint complex that takes into account all the relevant bio-realistic conditions and geometries would requires a great deal of CPU time and memory (Brilakis *et al.*, 2012), and this drives researchers to simplify their models. Therefore, in each stage of the FE modelling of the previous studies, structural shape and ways of anatomical segmentation, material properties, loading, contacts properties, and boundary conditions have been made which are show in Table 2-5 Objectives, methods, structures and simulation of human knee FEA model and Table 2-6 Loading and boundary conditions in human knee FE models.

Table 2-5 Objectives, methods, structures and simulation of human knee FEA models

References	Objective	Methods	Structural Assumptions	Simulation
(Bendjaballah, Shirazi-Adl and Zukor, 1995)	• Detailed reconstruction of a cadaveric total knee joint including bony structures (tibia, femur and patella) and soft tissue (ligaments, menisci and articular cartilage layers) • Finite element discretization of the reconstructed knee joint accounting for the articular surfaces needed for the non-linear contact analysis, the composite (nonhomogeneous) nature of the menisci, and the wrapping of the medial collateral ligaments around	CT	• Bones are considered to be rigid	Non-linear static analysis

References	Objective	Methods	Structural Assumptions	Simulation
	proximal tibia, various other ligaments, and the patella tendon for the quadriceps muscle group • Non-linear stress analysis of the model under various loads.			
(Bendjaballah, Shirazi-Adl and Zukor, 1997)	• To study the overall response, load transmission, role of ligaments and state of stress in various components under varus-valgus moments in the intact and collateral-deficient tibiofemoral joint are investigated.	CT	• Bony parts are rigid	Non-linear static analysis

References	Objective	Methods	Structural Assumptions	Simulation
(Donahue, Hull and Rashid, 2002)	• To develop a geometrically accurate 3D solid model of the knee joint with special attention given to the menisci and articular cartilage • To determine the extent to which bony deformations affect contact behaviour • To determine whether constraining rotation other than flexion/extension affects the contact behaviour of the joint during compressive loading	CT, Scion Image, MSC/PATRAN, TrueGrid, ABAQUS	• Bone is assumed to be rigid • Menisci are designed to be linear elastic and transversely isotropic	N/A
(Peña, Calvo, *et al.*, 2005)	• To develop a three-dimensional finite element model of the human tibiofemoral joint including the femur,	CT, MRI and I-DEAS V.9,	• Solid structure	Static analysis

References	Objective	Methods	Structural Assumptions	Simulation
	tibia, cartilage layers, menisci and main ligaments to estimate the contact areas and pressure distribution between menisci and articular cartilage and the stress distribution in the articular cartilage. • To investigate the effect of meniscal tears and meniscectomies on these variables	ABAQUS	• Bones are considered to be rigid	
(Peña *et al.*, 2006)	To analyse the combined role of menisci and ligaments in load transmission and the stability of the human knee	CT, MRI and I-DEAS V.9, ABAQUS	• Bones are considered to be rigid	Static analysis

References	Objective	Methods	Structural Assumptions	Simulation
			• Cartilage, menisci are linearly isotropic and homogeneous • Ligaments are hyperelastic and transversely isotropic	
(Shirazi and Shirazi-Adl, 2009)	To quantify the influence of alterations in osteochondral bone due to defects in the mechanics of articular cartilage and the entire joint.		• Bones are considered to be rigid	

References	Objective	Methods	Structural Assumptions	Simulation
			• Non-fibrils network is assigned for cartilage • Fibril network is designed for menisci	
(John, Pinisetty and Gupta, 2013)	To understand the effect of menisci on the stress and strain distribution in the knee joint.	MRI, ANSYS	• Bones are considered to be an elastic solid • Cartilage is linear elastic	N/A

References	Objective	Methods	Structural Assumptions	Simulation
			• Menisci are transversely isotropic elastic solid	
(Cartana et al, 2013)	To improve the quality of walking by minimizing the loads within the knee joint, on cartilage, and on the menisci.	CT, DesignModeler, ProEngineer, ANSYS	Elastic linear solid	N/A
(Kiapour *et al.*, 2014)		CT, MRI, 3D slicer image	• Bones, articular cartilage and menisci are linear elastic	• Quasi-static

References	Objective	Methods	Structural Assumptions	Simulation
			• Ligaments are anisotropic hyperelastic	
(Wang, Fan and Zhang, 2014)	To compare the stress distributions on knee joint cartilage between kneeling and standing positions	MRI, MIMICS ABAQUS	• Bone and cartilage are isotropic elastic • Menisci were modelled to be a transversely isotropic material • All ligaments are hyperelastic material	

References	Objective	Methods	Structural Assumptions	Simulation
(Sun *et al.*, 2016)	To use FE analysis to investigate the contact force and their location on the tibial plateau of an obese child with valgus knee and a healthy child.	CT, MRI, MIMICS, Rapidform XO3ABAQUS	N/A	• Static analysis

Table 2-6 Loading and boundary conditions in human knee FE models

References	Loading Condition	Boundary condition	Contact
(Bendjaballah, Shirazi-Adl and Zukor, 1995)	Compressive load ranging from 100-1000 N	• 6˚varus-valgus alignment was initially set • Tibia is completely fixed	• 7 frictionless nonlinear: ○ medial femoral condyle against the proximal medial meniscus, ○ medial femoral condyle against medial tibial cartilage, ○ distal medial meniscus against medial tibial cartilage, ○ 3 similar contacts were assigned to the lateral side. ○ The patellofemoral joint between the femoral cartilage

References	Loading Condition	Boundary condition	Contact
			and the retro-patellar articular cartilage
(Bendjaballah, Shirazi-Adl and Zukor, 1997)	Prior to the application of valgus-varus moments, the joint response was initially computed as being due only to the presented ligaments.	• 6˚varus-valgus alignment was initially set • 5˚flexion angle • The flexion-extension rotation was fixed on the femur at its initial position. • The femoral varus-valgus rotation along with the medial-lateral, anterior-posterior, and proximal-distal translation was set free.	• 6 potential frictionless contacts defined by a set of contactor and target surfaces. ○ In the medial compartment, the medial femoral cartilage against both medial tibial cartilage and the proximal surface of the medial meniscus, the distal surface of the medial meniscus against the medial tibial cartilage, 3 similar contact

References	Loading Condition	Boundary condition	Contact
		• The coupled internal-external rotation was either fixed or left unconstrained, • Tibia was completely fixed	zones were also assigned to the lateral compartment.
(Donahue, Hull and Rashid, 2002)	800 N compressive load	• Translation and rotation are fixed on the proximal femur • flexion/extension was constrained only in the base of tibia	• 6 contacts surface pair with frictionless with hard contact and finite sliding: femur and meniscus, Meniscus and tibia, Femur and tibia for both lateral and medial
(Peña, Calvo, *et al.*, 2005)	A vertical compression force of 1150 N	• On femur, flexion-extension, valgus-varus rotations were fixed • The lower surface of the tibia is fixed	• Menisci horn are attached to tibia plateau • medial meniscus is connected with medial collateral ligaments

References	Loading Condition	Boundary condition	Contact

			• 13 frictionless nonlinear contacts with finite sliding:
			  ○ 2 at the medial zone
			  ○ 2 at the lateral (femoral cartilage-meniscus and meniscus-tibial cartilage),
			  ○ 4 between the ligaments (LCL, MCL, PCL, ACL) and femur,
			  ○ 4 between ligaments and tibia
			  ○ 1 between cruciate ligaments

(Peña *et al.*, 2006)	• Compressional load of 1150 N and 134 N anterior-posterior	• Tibia and fibular are fixed • Femur was fixed with flexion-extension	• The ligaments were attached to bone • 15 frictionless contacts with finite sliding were defined:

References	Loading Condition	Boundary condition	Contact
	muscle load was applied to the femur • Load of 1150 N compressional load with a valgus torque of 10 Nm • Load of 1150 N compressional load with a valgus torque of 10 Nm adding the anterior load of 134 N muscle load		○ 2 at the medial zone ○ 2 at the lateral (femoral cartilage- meniscus and meniscus-tibial cartilage), ○ 4 between ligaments and tibia ○ 1 between cruciate ligaments and between the femoral cartilage and the retropatellar articular cartilage
(Shirazi and Shirazi-Adl, 2009)	1500 N compression force	• The base of the tibia is completely fixed	N/A

References	Loading Condition	Boundary condition	Contact
		• The sagittal surface of bony elements was restrained in the horizontal direction (i.e. medial-lateral and anterior-posterior) • the axial direction on the femur was left free	
(John, Pinisetty and Gupta, 2013)	A vertical force of 1150 N applied to the top of the femur surface in the direction of the joint	• Tibia is fixed • Rotation on the femur were fixed in all DOF.	• Femoral cartilage and tibial cartilage glued to the surface of the femur and tibia respectively • 4 frictionless contact pairs were assigned: femoral cartilage and femur, femoral cartilage and meniscus, tibial cartilage and tibia,

References	Loading Condition	Boundary condition	Contact
			and tibial cartilage and meniscus, and tibia cartilage with the meniscus • The menisci horn from both ends of the lateral and medial menisci is attached to the tibial cartilage
(Cartana et al , 2013)	800 N force is applied on the proximal head of the femur in the negative Z-axis direction	• Remote displacement is Z axis and Rotation around Y axis is allowed offset on the femur • On the distal head of tibia, the displacement allowing rotation around the Y axis was assigned	N/A

References	Loading Condition	Boundary condition	Contact
(Kiapour *et al.*, 2014)	• 0.50Nm of knee abduction with 25 degrees of flexion • 0-50 Nm of knee abduction+20 Nm of internal tibial rotation at 25 degrees of flexion • Baseline (no external loading, 0-50 degrees of flexion) • 15 Nm of internal tibial rotation (0-50 degrees of flexion)	N/A	• Frictionless surface-to-surface tangential with nonlinear finite sliding was as assigned to articular surface • 16 potential contact pairs: Femoral cartilage- tibia cartilage, femoral cartilage -menisci, menisci-tibia cartilage, femoral cartilage- patella cartilage, knee cruciate and collateral ligaments- femur, knee cruciate and collateral ligaments-tibia and ACL-PCL

References	Loading Condition	Boundary condition	Contact
	• 134 N of anterior tibial shear +15 Nm of internal tibial rotation (0-50 degrees of flexion) • All with the muscle load (quadriceps:400N and hamstrings: 200N)		
(Sun *et al.*, 2016)	• Load were applied to the distal end of the tibia and fibula • Knee joint angle and ankle joint angle were set according to kinematic results for natural walk	• The proximal end of the femur is fixed • Tibia and fibula bear the load of Ry_2 A plate was added on the distal end of the tibia and fibula	• Frictionless with finite sliding was assigned to femoral cartilage with tibia cartilage and femoral cartilage with the meniscus • Other contacts were applied as tied contacts to simulate the junction of the knee joint

References	Loading Condition	Boundary condition		Contact
(Wang, Fan and Zhang, 2014)	• Muscle force (quadriceps 215 N, Biceps 31 N and semimembranosus 54 N) • 1000 N compressional load	Kneeling model	• Femur is fixed • Tibia is set free • Ground plane was permitted to only move perpendicularly with other 5 DOFs restricted • the end of patellar tendon was constrained as it can only be displaced parallel to the direction of the femur	• The inner surface of all cartilages is tied to the corresponding bones • The two horns of the menisci were fixed to the tibial plateau. • Frictionless contact with finite sliding and hard contact surface-to-surface contact was set to the interaction between the cartilage and menisci and all possible contact relationship of the ligaments and bony structures, including contact between the patellar tendon and femur.
		Standing model	A rigid plane is tied to the end surface of the tibia Flexion angle is restricted with other DOF is unconstrained	

2.6. Conclusion

Although finite element (FE) studies of the human knee have increased our understanding of this vital structure, these computational models have not significantly contributed to alleviating adverse knee conditions such as osteoarthritis, the biomechanics of which remains a great and unanswered research challenge. This review chapter has provided an overview of modelling techniques in this field of research and has analysed the applicability of such studies in orthopaedic disorders. For this purpose, the major objectives, final achievements and study limitations of these FE models have been analysed. The main challenges faced in attempts to represent physiological and biomechanical conditions of the knee in modelling studies include (1) patient-specific modelling of different bones and soft tissues including ligaments, muscles, cartilage and tendons; (2) assigning bio-realistic loading conditions based on individualised and normalised physiological data, and (3) meticulous *in-vivo* validation of the FE simulation results. Based on the validated FE studies, the computational models can be implemented to ensure that they can provide reliable results either for patients suffering from disorders or for healthy patients, depending on the study's target population.

This literature review thoroughly explored and summarised the current understanding of the stresses within the healthy knee joint. On the other hand, the modelling of an OA knee joint by the finite element method has not been fully explored in the literature. Another research gap in the literature is the possibility of creating a finite element model of varus using moment; the literature mentions no methods other than changing the initial angle of the model.

In the literature, a model of the human knee joint with varus deformation has been created by changing the initial angle during model assembly, whereas the present thesis research would be useful in modelling a finite element model of OA and most importantly in terms of a new approach to creating a model of varus angle based on progressive deformation from the healthy knee. A major benefit is that the results of this study can be used to design or develop patient-specific designs for knee replacements, braces and prostheses.

In this thesis, two finite element models of the knee will be developed ~~in this research~~: one of the healthy knee and another of the OA knee which shows articular cartilage and menisci damaged by OA. These two models will be tested, and the results will be compared. The results will also be validated ~~with~~ against the results of other researchers who used the same test methods. Varus-valgus OA knees will be evaluated by changing the knee bones' angles. This can be achieved by examining the stress in knee cartilage when the knee angles are changed so that it is possible to understand the differences between the behaviour of healthy knee and that of the OA knee.

3. Methodology

3.1. Introduction

The objectives of this research are to create and validate a general-purpose computerised knee joint model and to use this FE model to analyse and evaluate the results. This can be achieved by using MRI (Magnetic Resonance Imaging) scan of a healthy subject to provide an accurate geometry, from which the finite element model will be created. Two models of the knee will be developed by using FE models in this research. One will be a model of a normal healthy knee while the other will represent an OA knee suffering articular cartilage and menisci degenerated by OA. These two models will be tested, and the results will be compared with each other. The finite element analysis will be done using ABAQUS software (ABAQUS Inc., USA).

3.2. Medical Imaging and Construction of a 3D Knee Model

There are three mains steps in developing a 3D finite element knee model, which are pre-processing, simulation and post-processing. In pre-processing a CT/MRI image is needed to show the spatial relationships of the elements (Sun *et al.*, 2005). To achieve the knee joint finite element model, its three-dimensional structure must be reconstructed. The human knee is a complex joint which act as the hinge of the leg and connects the upper leg and lower leg together. A practical model cannot be designed with only the Computer Assisted Design (CAD) techniques. So, it is a challenging and time-consuming task at this step to construct the irregularly shaped 3D geometric structures of the knee profile elements. Some other software is required to create a versatile topological structure of the human knee before starting the simulation.

The MRI scan subject was a male volunteer athlete. The MRI was done within the Medical School, University of Exeter. The MRI input data files were processed to create a three-dimensional model. In pre-processing, different knee segments were constructed; these parts were smoothed and then assembled according to their actual three-dimensional spatial relationships.

The second step, simulation is the actual process of finite element modelling, consisting of geometric assembly, definitions of material properties, assigning interaction, contacts boundaries, boundaries conditions and loading to the model. After the simulation, the results are analysed. Then, the final step or the post-processing step is carried out, both to validate the results of the experiment and to supply the solutions to research problems (Sun *et al.*, 2005).

The early studies (see Table 2-5) usually presented a simplified human knee models, but the use of modern medical imaging techniques has enabled scholars and engineers to model a more detailed bio-realistic structure of the knee. These models are generally based on multiple 2D image slices processed by self-developed code or commercial software such as Slicer3D (Jin, 2014), Simpleware (Fontanella *et al.*, 2012), 3D Doctor (Jin, 2014), MIMICS (Flavin *et al.*, 2008; Qian, Ren and Ren, 2010) or AMIRA (Cheng *et al.*, 2008). Although bone geometries are mainly constructed from CT images, MRI is sometimes used for this purpose if finer segmentation is required (Jin, 2014).

In the CT data, tissues can be differentiated through contrast segmentation based on the grey-scale value of a voxel. A voxel is the smallest three-dimensional element in an object which can be distinguished during the scanning process (Wei *et al.*, 2010). Therefore, CT is more effective for modelling hard tissue and

even for modelling the boundaries between bones and soft tissues than using MRI (Wei *et al.*, 2010). For the soft tissues, on the other hand, MRI can be the best option as the CT data image resolutions are not sufficient to differentiate and segment these structures. MRI is used for this type of imaging due to its ability to provide high-contrast images of soft tissues. It is important to note that this technique is both non-radioactive and non-invasive and can capture cross-sectional structural images. MRI captures images on the basis of the changes in orientations of the magnetic moment of the hydrogen nuclei for each specific tissue which are generated by placing the tissue in a magnetic field and stimulating it with radio frequency waves (Nigg and Herzog, 2007). After this, a receiver coil measures the signal-decay, processing and providing an image which presents the area of the scanned object (Nigg and Herzog, 2007). Even though the CT is most preferable for the hard tissue, in this research, both hard and soft tissues were extracted using MRI.

After the medical image processing was done, the next step was to collect slices of 2D images from MRI. The data were displayed as two-dimensional grey value images and were obtained in Digital Imaging and Communication in Medicine (DICOM) format. DICOM is a file format used in the medical sector. It must be converted in order to be compatible with the ABAQUS (using other engineering software packages, such as SOLIDWORKS). Each segment was exported as a separate file for further refinement regarding geometric construction. Computer Aided Design (CAD) is the option which can be used for this purpose for further surface smoothing or to increase the model accuracy (Sun *et al.*, 2005; Morales-Orcajo, Bayod and Barbosa de Las Casas, 2016). SOLIDWORKS (Yu *et al.*,

2008) or CATIA (Antunes *et al.*, 2008) are the two main software packages that are most commonly used for the CAD process while others such as Unigraphics, Pro/Engineering and Rhinoceros are reported as well (Jin, 2014). A roadmap from CT/MR images to the 3D reconstruction is presented in Figure 3-1.

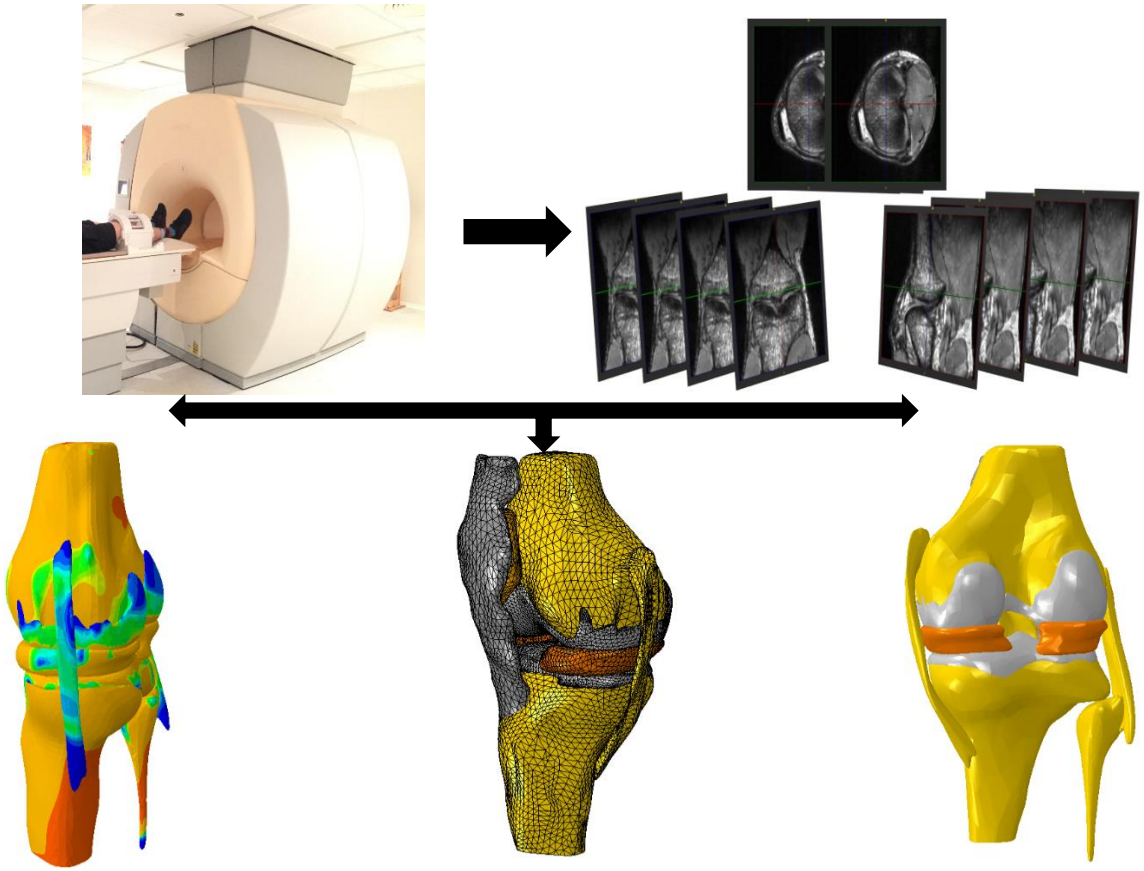

Figure 3-1 Bio-CAD MRI based technique for modelling the human knee

The image-based Bio-CAD modelling technique has been widely used in several types of research by using different methods (Sun *et al.*, 2005). The three-dimensional model can be constructed by segmenting 2D images into a 3D model. After a 3D model was constructed, smoothing or cleaning process was done. This step has been done to achieve a clean 3D model (Figure 3-2).

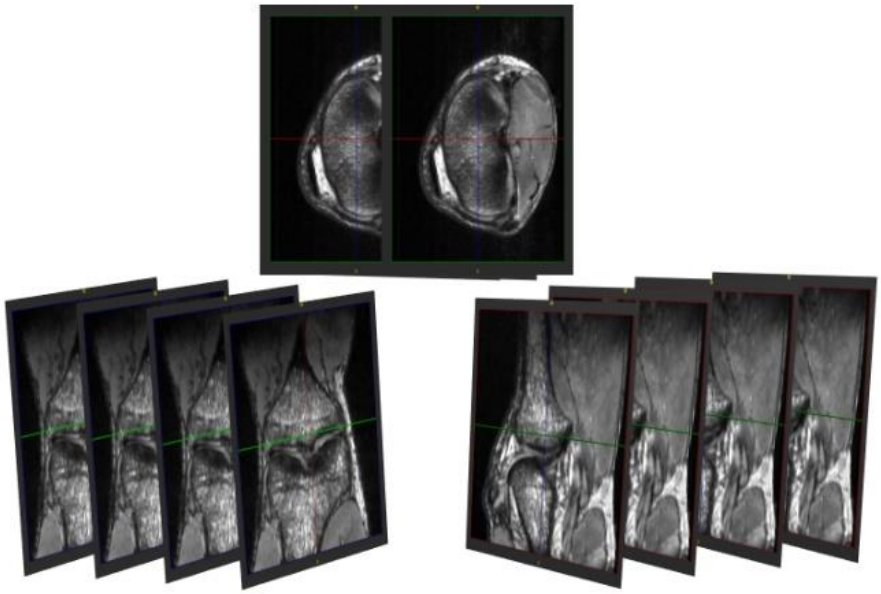

Figure 3-2 CAD model construction using MR images data collection (segmentation of 2D images)

3.3. Three-dimensional geometric construction

To create a full 3D model of the human knee joint, the spatial relationships are extracted from the DICOM files, which show the images in 3 planes: the sagittal, coronal and transverse planes. The MRI scans were performed with the collaboration of a staff member of the Medical School of the University of Exeter. The MRI scanner that was used was a 1.5 Tesla Phillips Intera system using T1 3D Gradient Echo sequence (TR/TE = 57 ms/21 ms, spatial resolution with a voxels size of 0.7 × 0.7 × 0.7 mm^3) (**Error! Reference source not found.**). This complex bio-realistic model of a knee joint was reconstructed from medical MR images of a subject with a healthy knee. Three MRI scans were done on two healthy male athlete subjects with no history of lower limb extremities having interval separation of 1.5 mm in sagittal, coronal and axial planes with 0° of knee flexion. Both subjects were between the age of 20 and 25. Subject A had a height

of 189 centimetres and weight of 85 kilograms and subject B had a height of 166 centimetres and weight of 70 kilograms.

The first two scans were done on subject A. The first scan focused only on the joint not the bone and the resolution of the images was low. The image quality of the first scan was 288 by 288 by 100 slices. The spacing between each slice in the X and Y directions was 0.46 millimetres and in the Z direction was 1 millimetre (Figure 3-3). The image was too blurry, and hence it was not possible to differentiate the parts from one another. Thus, this MRI result could not be used to extract and threshold the model into a proper shape.

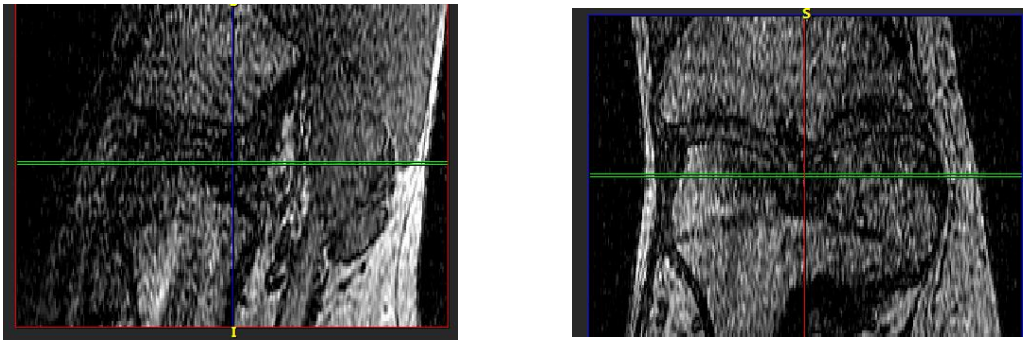

(a) Sagittal plane (b) Frontal plane

Figure 3-3 First MRI scan result of subject A (a) Sagittal plane (b) Frontal Plane.

A second MRI scan was performed on subject A, but the result of this scan was too short in length (as shown in Figure 3-4), even though the quality of the image was better and clearer than the first scan.

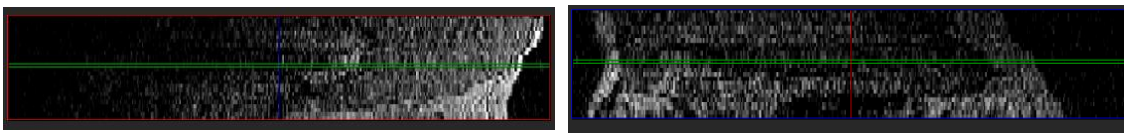

(a) Sagittal plane (b) Frontal plane

Figure 3-4 Second attempt on MRI result of Subject A (a) Sagittal plane (b) Frontal Plane.

A third scan was performed on subject B. The quality of this scan was better, and it had a better image quality than the first two scans. The resolution of this scan was 648 by 648 by 250 slices. The spacing in X and Y directions were 0.2 and in Z direction was 1 millimetre as shown in Figure 3-5.

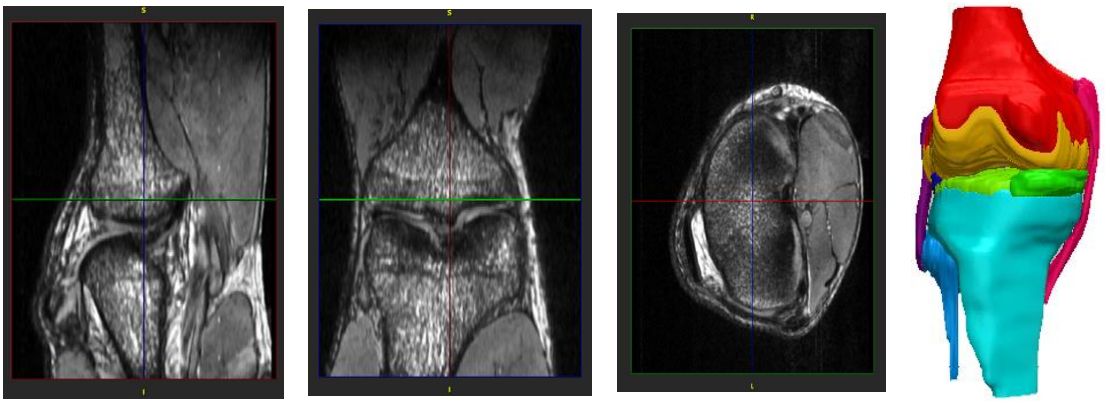

(a) (b) (c) (d)

Figure 3-5 The third MRI scan from subject B, (a) sagittal plane with anterior on the left and posterior on the right, (b) a frontal plane with medial on the left and lateral on the right, (c) a transverse plane with anterior on the left and posterior on the right with medial on the top and lateral at the bottom, (d) a 3D model of reconstructed from the MR images.

The segmentation and thresholding of each part, including femur, tibia, fibula, ligaments, patella, patella tendon, menisci and cartilages were done using

SCANIP software (Synopsys, USA). The segmented parts were then exported and assembled to form the three-dimensional FE model of the knee joint.

3.4. Gait Analysis

3.4.1. Movement of the Knee Joint

To explain the relative positions and movements of the knee joint it is necessary to understand the anatomical plane which were explained previously in Chapter 2: Figure 2-2.

The sagittal plane divides the body vertically into its right and left halves; the frontal (or coronal) plane divides the body vertically in its anterior and posterior halves; the transverse (or axial) plane divides the body into its inferior and superior halves.

There are six degrees of freedom of the knee (Figure 3-6). They can be defined: in terms of three translations and three rotations. The three translations are anterior-posterior, medial-lateral, and proximal-distal; and the three rotations are flexion-extension, internal-external (medial-lateral), and varus-valgus (adduction-abduction) (Woo *et al.*, 1999)

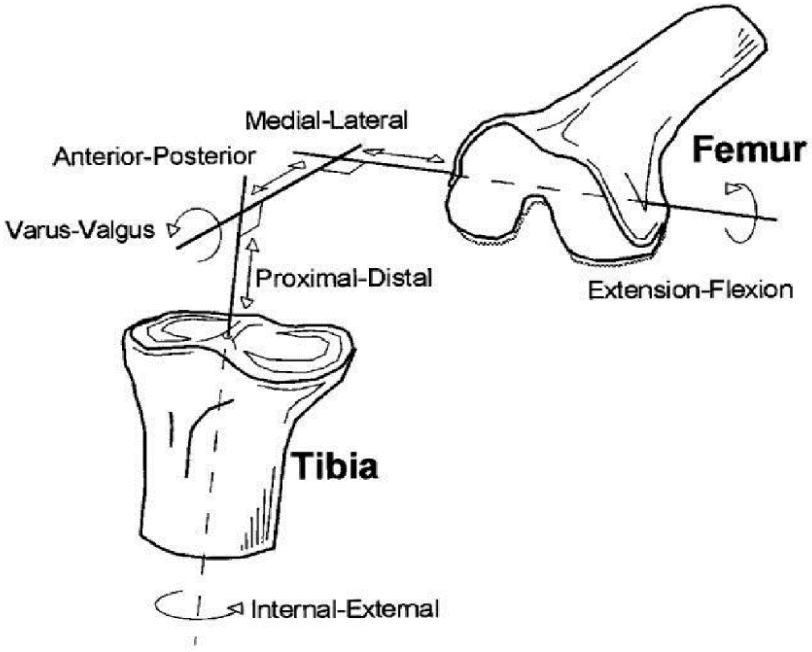

Figure 3-6 The six degrees of freedom of the human knee joint (Woo *et al.*, 1999)

Figure 3-7 illustrates the movement of the mechanical axis of the lower extremity compared to the ground surface. The mechanical axis of the leg is defined as the line that connecting the centre of each joint from the hip to the knee down to the ankle.

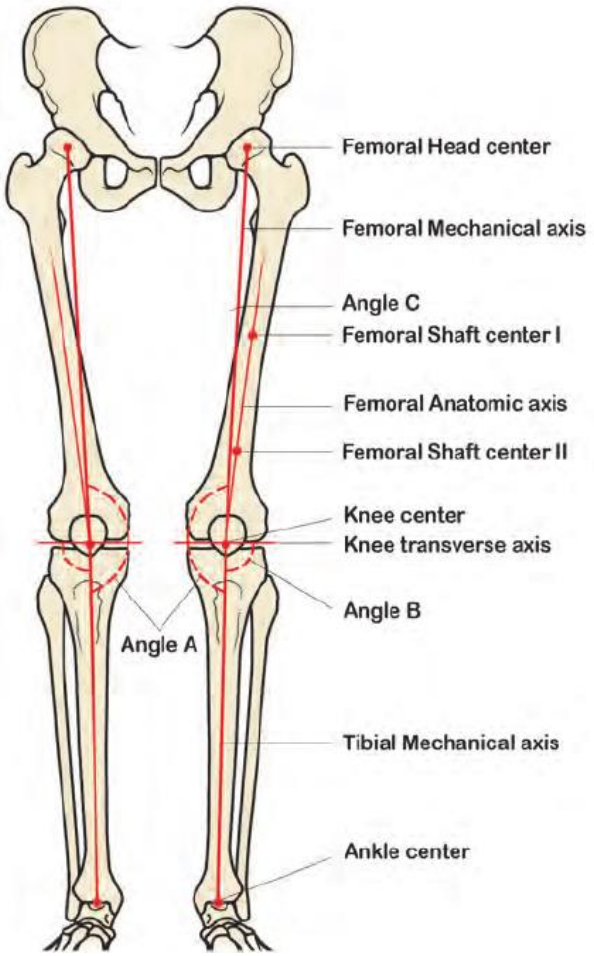

Figure 3-7 Mechanical axes of human lower extremity (Fosco *et al.*, 2012)**.**

3.4.2. Elements of the Knee Joint and Movement Control

When the knee joint is in action, hip, knee and foot work together. The knees provide flexible but stable support for the body. The various structural elements of the knee joint (i.e., bones, cartilage, muscles, ligaments, and tendons) enable the knees to do their job.

As mentioned in chapter 2, menisci are important for reducing contact stresses on the articular cartilage, shock absorption, circulation of synovial fluid and joint stability (Marieb *et al.*, 2013), while ligaments including tendons and joint capsules stabilise the joints of the skeletal system. The function of ligaments is

to connect bones to other bones, provide stability to joints by guiding joint movements and to prevent excessive joint motions. The kind of movements depends not only on the form and structure of the articulating bones but also on the ligaments incorporated into the articular capsule. (Ethier and Simmons, 2008).

3.5. Experimental data with motion capture system with force plates

For many decades, cinematography has been the most common measurement technique in the analysis of human motion (Angulo and Dapena, 1992). In order to make a detailed analysis of an individual movement pattern, the technician would usually take video records of sport and exercise activities and analyse the data (Payton and Bartlett, 2007).

Camera-based systems with reflective markers are the most precise systems for gait analysis (Allard, 1997). In the laboratories of gait analysis, the ground reaction force (GRF) is also measured using force platforms which typically record from only one or two steps of the gait depend on the size of the platform. There are three other common methods in collecting human movement data: electrogoniometers, electromagnetic tracking devices, and optoelectronic measuring systems. Ultrasound is an alternative method to camera-based systems (Kiss, Kocsis and Knoll, 2004) and magnetic tracking systems (Kobayashi *et al.*, 1997), which enable the analysis of human movement in a complete 3D kinematic system, have also been used.

Over the last decade, many novel methods have been developed for gait analysis systems, for example, laser technology and measuring near-body air flow (Pallejà

et al., 2009) in order to measure kinematics and spatial gait parameters. Also, electronic carpets and wearable force sensors can be used for estimation of ground reaction forces, the centre of pressure, and temporal gait parameters (Liu, Inoue and Shibata, 2010).

Portable body-mounted systems are another novel method that has been used in data collection for human motion analysis (Allet *et al.*, 2010). This method can collect the data over more steps, and kinematic data such as joint angles, accelerations, and angular velocities of the body segments that carry the sensors can be measured directly using the portable systems. Joint angles can also be measured with various electrogoniometers (Zheng, Black and Harris, 2005).

In the present thesis research, a force platform and motion sensors were used to capture the data.

3.5.1. Equipment used in gait analysis data collection

The kinematic variables analysed in this gait study were captured using equipment from Codamotion (2018); the equipment that was used in this data collection for gait analysis is listed below. The detail and limitation of each components are available on Codamotion (2018).

- Four 3D Camera scanners (CX1183 3D camera scanner) (Figure 3-9 (a))
- Marker, Cluster and Drive boxes (Figure 3-9 (b and c))
- Microgate Light Gates (Figure 3-8)
- Force Platform (Figure 3-10)

(a) (b)

Figure 3-8 (a) Photocells (b) Reflectors

(a) CX1183 3D camera (b) Marker Drive box

(c) Cluster

Figure 3-9 (a) 3D Camera scanner (b) Marker Drive box (c) Cluster

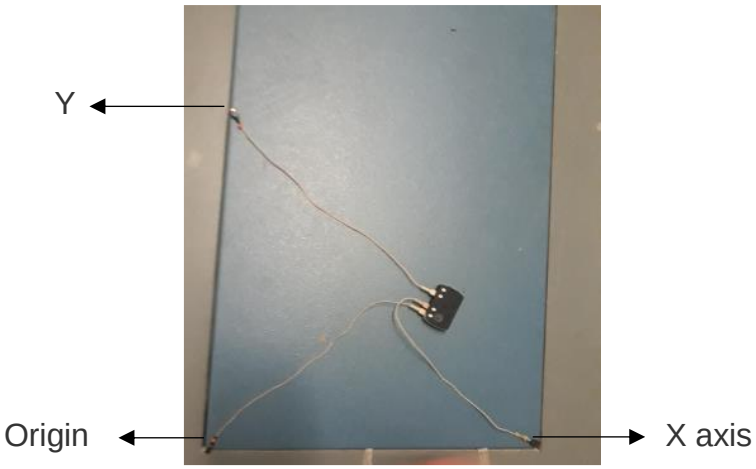

Figure 3-10 Force plate alignment

Preparations are needed at the beginning of each session of the experiment. The force plate must be alignment and zeroed. This allows positional information to be linearly transformed. The drive boxes and clusters must also be prepared. This preparation was done so that each of the markers on the subject are numbered corresponding properly to the assigned marker profile. To position the markers accurately, a sufficient knowledge of lower leg anatomy is required These preparations are essential for the motion analysis system to accurately compute joint moment and angles. The detail of the position of each clusters and drivers are shown in

Table 3-1, while Figure 3-11 shows the position of where the components were attached to the subject. These details are taken from the Codamotion User Guide (2018).

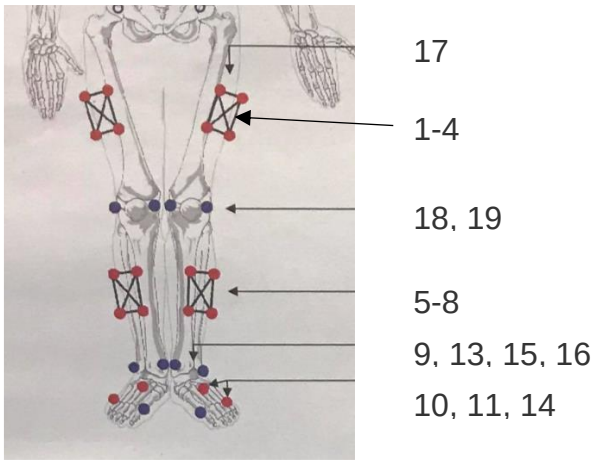

Figure 3-11 Marker placement diagram (Grimes, 2018)

Table 3-1 Marker Placement

Equipment	Marker Number	Marker location
Clusters	1-4	Thigh
	5-8	Shank
Driver Box 1	9	Heel
	10	5 Metatarsal
	11	Top of the foot
Driver box 2	13	Calcaneus
	14	1st Metatarsal
	15	Medial Malleolus
	16	Lateral Malleolus
Driver Box 3	17	Greater Trochanter
	18	Lateral Knee
	19	Medial Knee

3.5.2. Data Collection and Processing

Motion Analysis and Testing

The experimental set-up can be seen in Figure 3-12. The blue rectangle is the force plate which is surrounded by four Coda CX1 cameras, light gates, and reflectors which are placed in between each camera with a sufficient distance before and after the plate. The subject was asked to maintain a normal gait during the data collection. All other sensors in the room were put in boxes during testing to avoid interference.

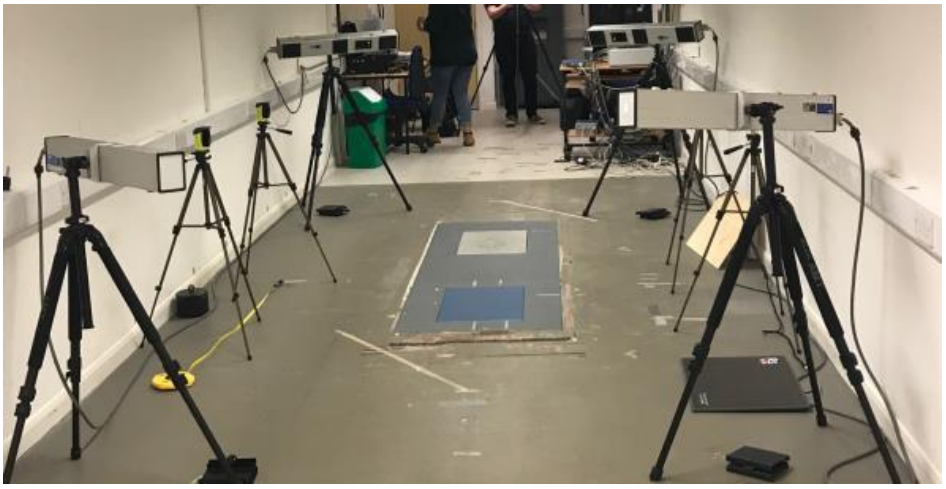

Figure 3-12 Experimental set up

3.6. Experimental data collection using motion sensors and force platform results

The data for this experiment was taken using a force platform and motion sensors and was collected by Grimes (2018) with the help of the College of Sport and Health Sciences, University of Exeter (St. Luke's campus). The results that were obtained from the experiments are presented in Figure 3-14, Figure 3-15, and Figure 3-16. To understand the results obtained from the experiment of gait

analysis, knowledge of the gait cycle is necessary. In single stance, it is divided into 5 phases i.e. heel strike, early stance, midstance, late stance and toe off (Figure 3-13). In this thesis, the focus will be on the midstance phase of the gait.

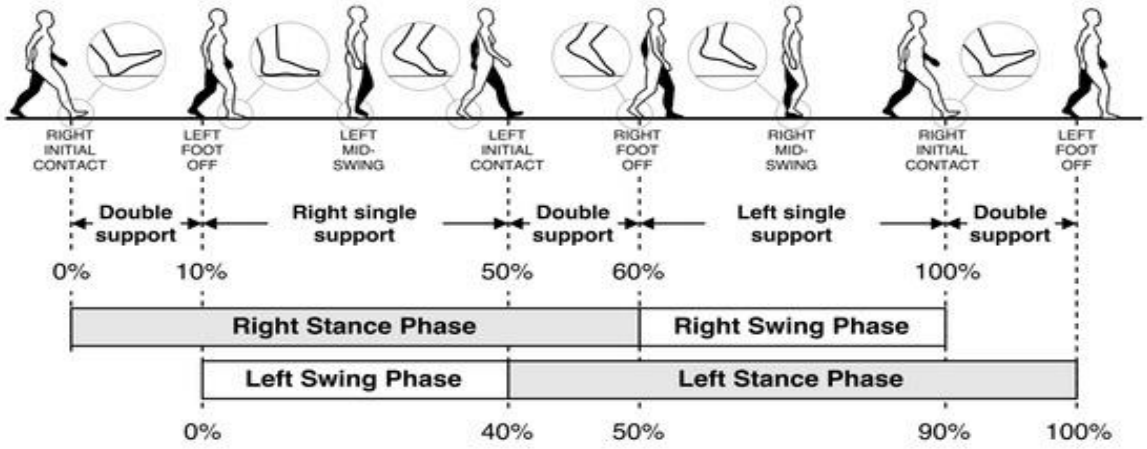

Figure 3-13 Gait cycle (Tunca *et al.*, 2017)

The experiment was done 10 times repeatedly to study the pattern of the gait. This was to validate the loading for the finite element simulation. The data that were obtained from the experiment were knee flexion angle, knee flexion moment and ground reaction force. The GRF at midstance (i.e., at 25% of stance phase) that were recorded from all 10 trials are all at 800 N which is as expected. Therefore, 800 N will be used for loading the model in the FE analyses.

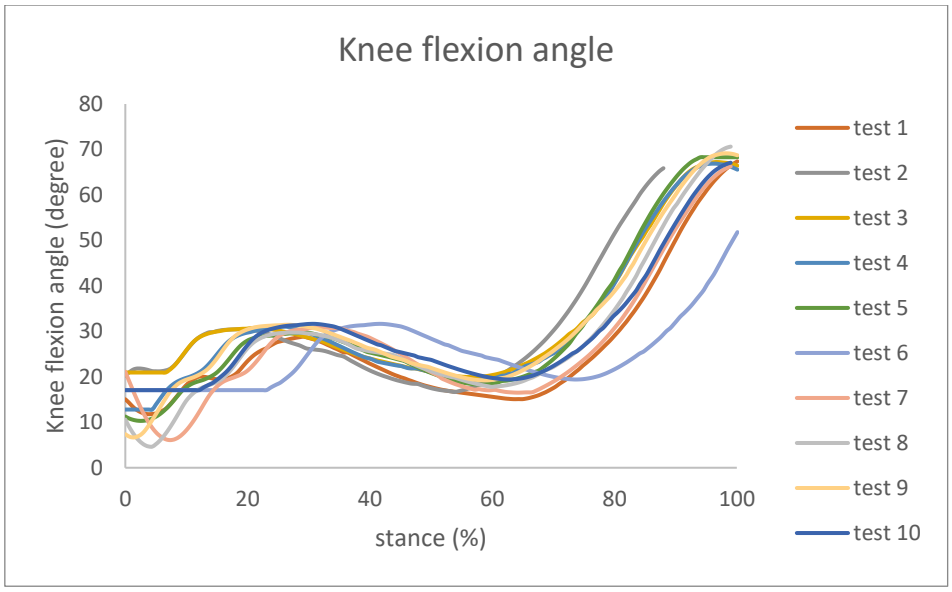

Figure 3-14 Knee flexion angle during stance

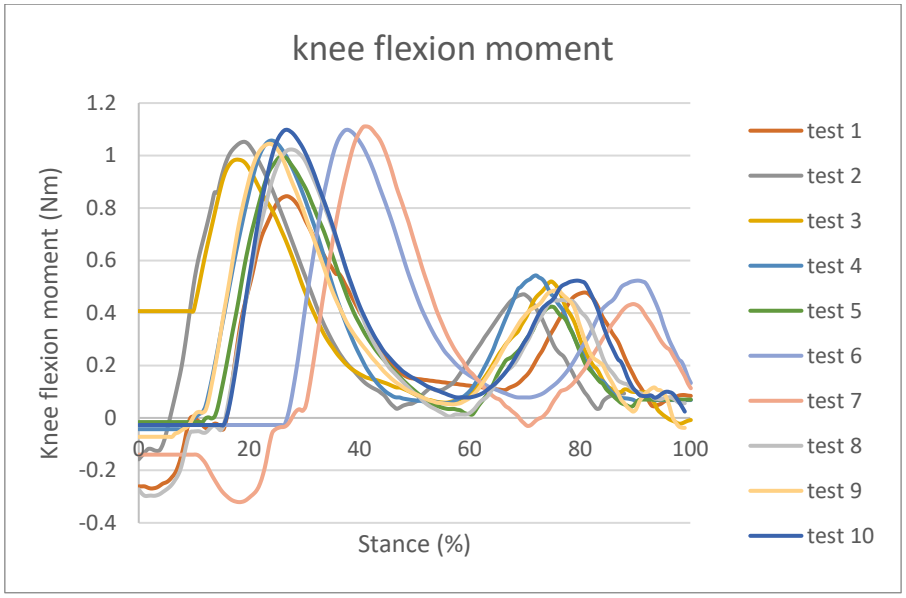

Figure 3-15 Knee Flexion moment during stance

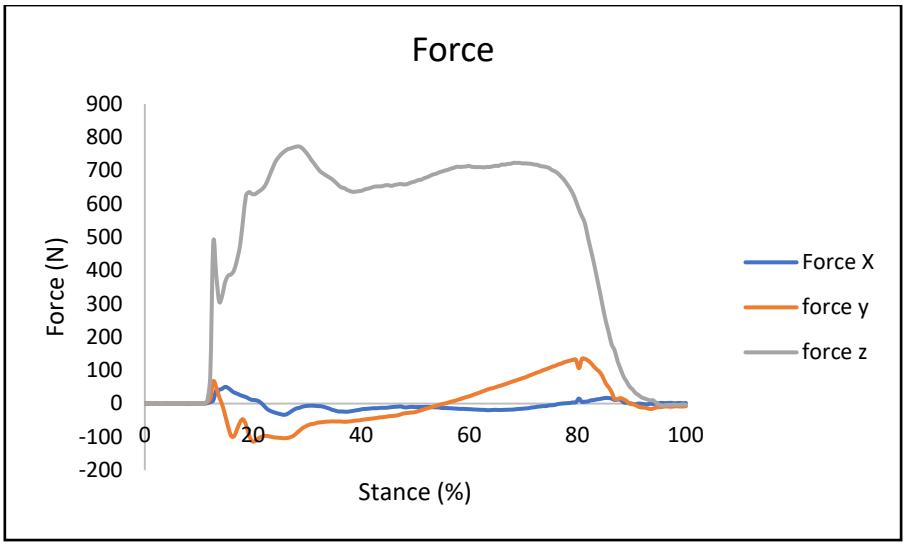

Figure 3-16 Force VS. Stance gait pattern using a motion sensor and force plate

3.7. Conclusion

In the data collection using the force plate, the maximum force that occurred within the knee joint was 800 N. This 800 N ~~force~~ load is equivalent to the human body weight of 80 kilograms which is an average body weigh that has been used in many analyses. This result is also similar to the load that was used in several studies, for example Donahue, Hull and Rashid (2002), Zielinska and Haut Donahue (2006), Cartana et al (2013) and Tarniţă et al (2014). This 800 N ~~force~~ loading will then be used in the analyses in this thesis.

4. Finite element model construction

4.1. Introduction

Finite Element Analysis (FEA) is used in a wide range of situations, from solving stress-related issues to modelling the collapse of an entire building. The analysis can be set to be in 2D, 3D, or even in an asymmetrical model. The main benefits of using FEA is that it is cost effective, as running an analysis using this computational method is cheaper than performing a physical experiment. Moreover, computational analysis can deal with complex constraints as well as time, frequency, and dependent loading.

In this thesis, a three-dimensional finite element model of the tibiofemoral joint cartilage, menisci and ligaments was created. After the segmentation and smoothing in ScanIP, each part was exported to ABAQUS in separate files. The parts were then assembled (as shown in Figure 4-1).

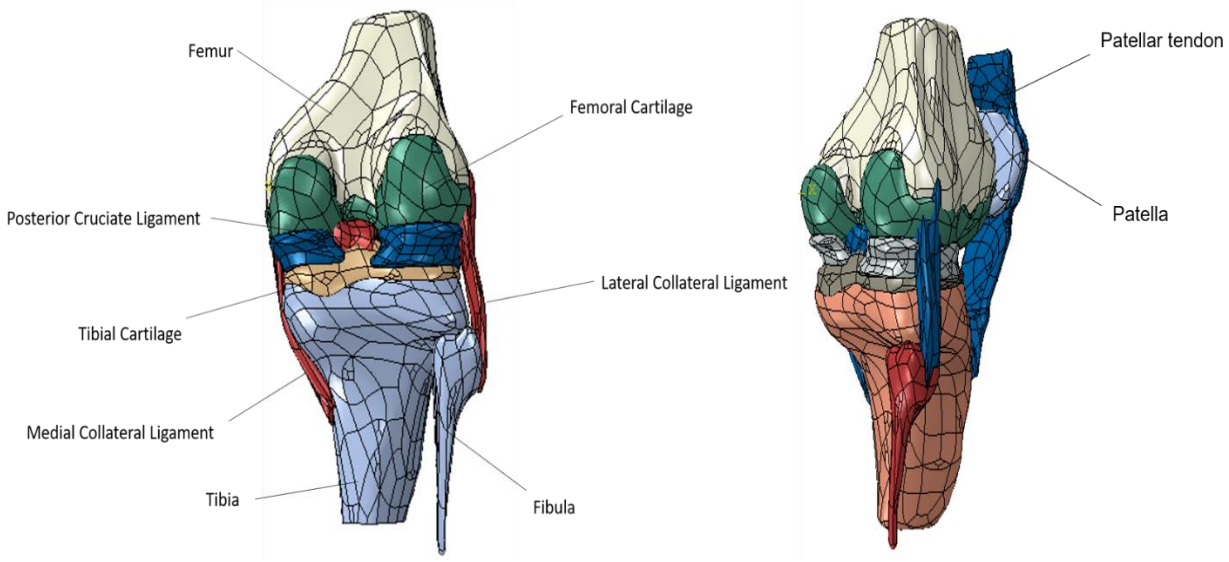

Figure 4-1 A complete model of the knee complex

The parts are imported into ABAQUS and combined into a single part with combine into a single part option. After imported the model into ABAQUS, it can be seen that the parts overlap each other. To create a model that can be analysed, these overlaps must be removed. The process of removing theses overlaps can be done using the connecting part to cut out the overlaps to achieve the desired geometry of the joint in the FE model.

In this model, the cartilages overlap the bones, and the menisci are overlap the two cartilages. Thus, the bones were used to cut out the overlap with the cartilages, and the cut cartilages were used to cut the overlap with the menisci. After the overlaps were removed, each part was assigned material properties, contact boundaries, loading, and boundary conditions.

4.1.1. Material properties

The material properties that are assigned to each of the knee joint components in the literature are varied and, in some research, the bones are even taken to be rigid. The material properties used in this thesis are shown in Table 4-1. These material properties were taken from Peña et al. (2005 and 2006), and Cartana et al. (2013).

Table 4-1 Material Properties used in the analysis

Geometry	Young's Modulus (E) [MPa]	Poisson's Ratio (v)
Femur	18600	0.3
Tibia	12500	0.3
Cartilages	12	0.45
Meniscus	59	0.49
Ligaments	10	0.49

4.1.2. Contact Properties

In the literature, up to 15 contacts have been assigned to the knee models. All these are surface-to-surface contacts with finite sliding (Donahue, Hull and Rashid, 2002; Cartana et al, 2013; Tarniţă et al, 2014). The contact information from the literature is presented in Table 2-6.

To define the contact relationships between the different knee components in this research, a total of 4 surface-to-surface contacts were assigned in the model. Two of the contacts were assigned to the bones and their cartilages. The other two contacts were assigned to the outer surfaces of the cartilages which contact the menisci on both femur and tibia sides, and the ligaments were bonded together with the bone.

4.1.3. Loading and boundary conditions

In the literature on knee models, there are different ways to apply load and boundary conditions (Cartana et al, 2013; Tarniţă et al, 2014). This thesis set conditions according to the simulator and gait patterns (see Table 2-6).

This research simulated the model based on the midstance phase of the gait where the foot is fully in contact with the floor and the knee joint is fully extended. The boundary conditions assigned to the model were taken from the literature: the model was fixed at the distal end of the tibia to replicate a standing or a fully extended single midstance phase. Zero displacements in the x and y directions were assigned to the femur preventing the bending or flexion of the joint. A load of 80 kilograms, or 800 N concentrated force, was applied from the top of the model, in order to replicate the body weight of an average male athlete.

4.1.4. Mesh generation

In order to create a finite element model of a human knee, it is necessary to study the structure and geometry of the knee, including biomechanical functions and materials.

The knee joint is composed of a variety of structures and soft tissues: bones (femur, tibia, fibula and patella), articular cartilage, meniscus, and ligaments (Figure 4-2). These elements have their own functions with different materials and structures.

Because these components come in different shapes and sizes, and have vastly different properties, the distinct size of the mesh was varied depending on the

element being modelled. Therefore, the main focus being on cartilage and menisci, a finer mesh size was generated for these than for the bones.

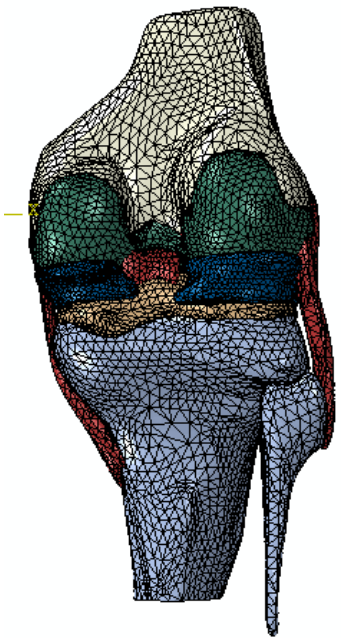

Figure 4-2 Meshed distribution geometry

4.1.5. Mesh Sensitivity Studies

As there was a limitation on the maximum number of nodes (and degrees of freedom) available in the ABAQUS teaching licence, a mesh sensitivity analysis was carried out on each part of the model to find an optimum mesh size for the most accurate overall results. This optimum mesh size for each components of the model was then used in the analysis presented in the next section.

The mesh sensitivity analysis was carried out by considering each of the following components separately: femur, tibia, cartilage, and menisci. As mentioned above, a constant force of 800 N was applied to the top of each part, while the bottom of each was fixed. As the global mesh size was altered, the effects of the mesh

density on the maximum von Mises stress was taken into consideration. The results of the mesh sensitivity analysis are presented in Figure 4-3.

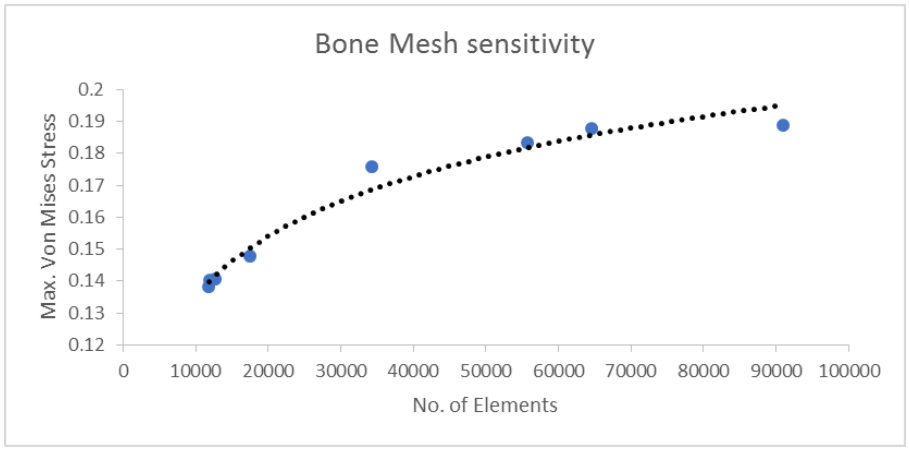

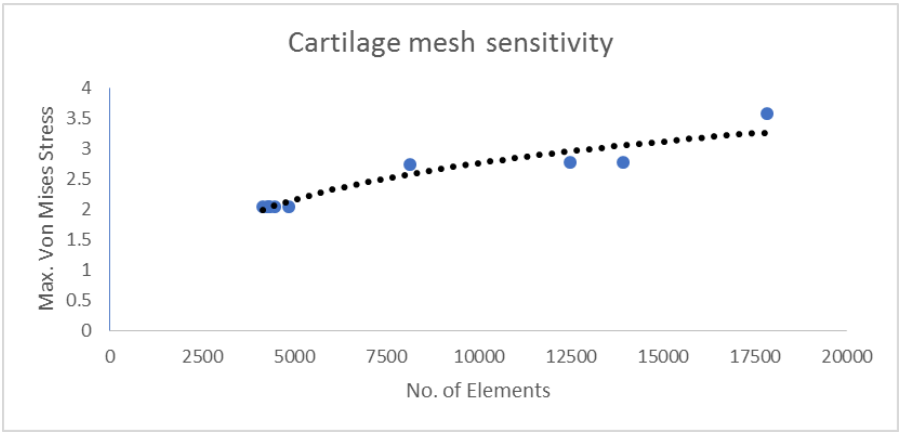

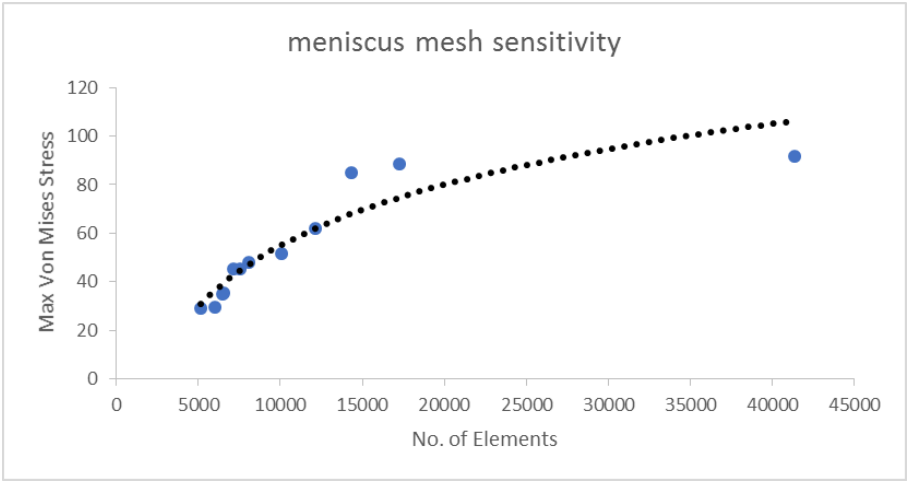

Figure 4-3 Mesh Sensitivity study for each part of human knee joints

The main focus of this thesis is the cartilage and meniscus, and thus the mesh sizes of these two parts are very dense. Mesh sizes and densities, and the number of elements assigned to each component of the model, were determined through careful analysis of the mesh sensitivity studies presented in Figure 4-3. The mesh size was selected based on the trendlines in the sensitivity analysis (dotted lines in Figures 4-3).

As the bones are the major part of the joint (then the cartilage and menisci), the majority of the FE elements would be on the bones. The bones will have a large global mesh size while the cartilage and meniscus will have a finer mesh size. The assigned number of elements and element types for the final (optimal) mesh are shown in Table 4-2.

Table 4-2 Element type and number of elements that was assigned to each component of a healthy knee

Component	Element Type	Number of Elements
Femur	Quadratic Tetrahedral	47,588
Tibia and Fibula	Quadratic Tetrahedral	35,160
Cartilages	Quadratic Tetrahedral	23,767
Menisci	Quadratic Tetrahedral	13,666
Ligaments	Quadratic Tetrahedral	11,236

4.2. Results

The material properties and boundary conditions used in this research were based on Tarniţă et al. (2014). The model was extracted from MR images and used to construct a complex 3D geometric structure. All the components, including bone structures (femur, tibia, fibula), their cartilages, menisci, and ligaments were included. All the components were assigned elastic material properties as shown in Table 4-1.

Two analyses were done by Tarniţă, Catana and Tarnita (2014) who had applied loads of 800 N and 1500 N on the proximal head of the femur. A displacement which allows offsetting in the Z axis and also allows rotation around the Y axis was assigned to the femur head. These boundaries were assigned to allow movement of the hip. On the distal end of the tibia, the displacement was set to zero, and rotation around the Y axis was allowed in order to simulate movement at the ankle around the tibia (Figure 4-4).

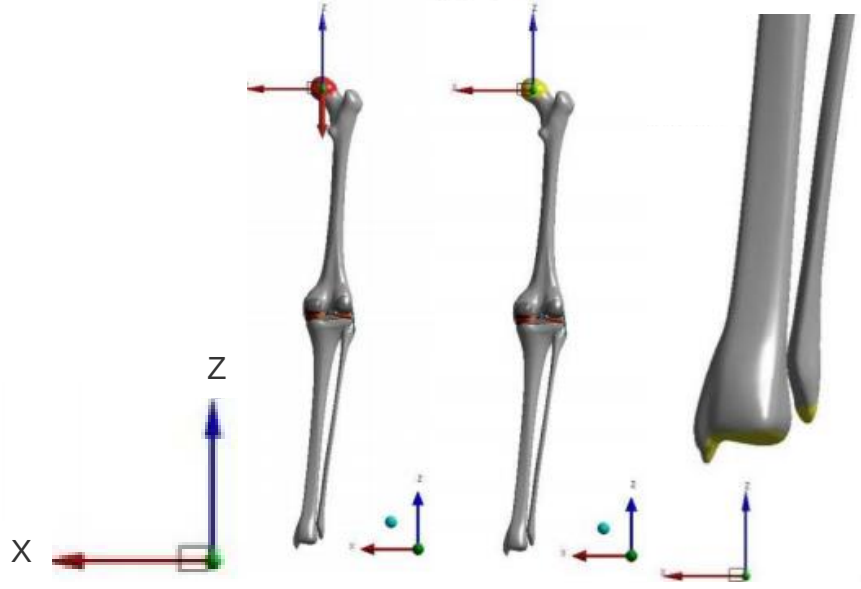

Figure 4-4 Load and boundary conditions determined based on Tarniţă et al. (2014)

The model for this research analysis was extracted from the MRI. The model extracted consisted of all bony structures (femur, tibia and fibula), cartilages, menisci and ligaments (cruciate and collateral). As mentioned earlier, elastic material properties were assigned to each component of the knee joint in the model, as shown in Table 4-1, which are the same as the material properties used by Tarniţă et al. (2014); even though the models were not the same, the boundary conditions were set to be the same. The base of the tibia was set to be fixed, and the same load was applied to the top surface of the femur. The maximum von Mises stresses that were reported in Tarniţă et al. (2014) for 800 N load on the healthy knee model were 2.14 MPa, 2.17 MPa, and 2.12 MPa at femoral cartilage, tibial cartilage, and menisci respectively. For 1500 N loading, the stresses that were presented were 4.53 MPa, 3.22 MPa and, 3.31 MPa at femoral cartilage, tibial cartilage, and menisci respectively.

As mentioned earlier, the model in this research considered a fully extended knee joint or standing position. The load was applied at the top of the model and the distal base of the model was fixed. The simulated results are presented below. The undeformed and deformed models are shown in Figure 4-5. The results show that the deformation occurs on the lateral side of the knee joint, causing the menisci to be squashed and to slide to the side.

Regarding validating the model, it must be noted that the human knee is a complex joint, and human knee are different from one another due to many reasons, e.g. the shape of the bone, density of the bones, and the gender of the subject. Thus, it is impossible to validate the model in the traditional sense.

The maximum stresses that were measured from the FEA for 800 N loading were 2.76 MPa, 1.624 MPa, and 4.808 MPa on the femoral cartilage, tibial cartilage and menisci respectively (see Figure 4-6). The stress distribution of each component is different, on the femoral cartilage, the maximum stress that was measured occurred in the centre of the cartilage, while on the tibial cartilage the maximum was on the lateral-posterior side. On the other hand, on the menisci, the maximum stress occurred at the lateral-anterior side.

For the loading of 1500 N, the stress distribution and location of the maximum stress on each component changed. The measured maximum stresses at 1500 N load were 2.796 MPa, 2.939 MPa and 7.441 MPa on femoral cartilage, tibia cartilage and menisci respectively (see Figure 4-7). In both cartilages the maximum stress occurred at the lateral-posterior side while on the meniscus, the maximum stress occurred on the lateral-anterior side.

The maximum von Mises stress results measured in the analysis with an 800 N ~~force~~ load on the femoral cartilage was 2.76 N, which is 0.62 N greater than the result presented in Tarniţă et al. (2014). The maximum that this model predicted with an 800 N load on the tibia was 1.642 N, which is 0.546 N less than what is presented by Tarniţă et al. (2014).

The simulated results of 800 N and 1500 N are shown in Figure 4-6 and Figure 4-7 respectively.

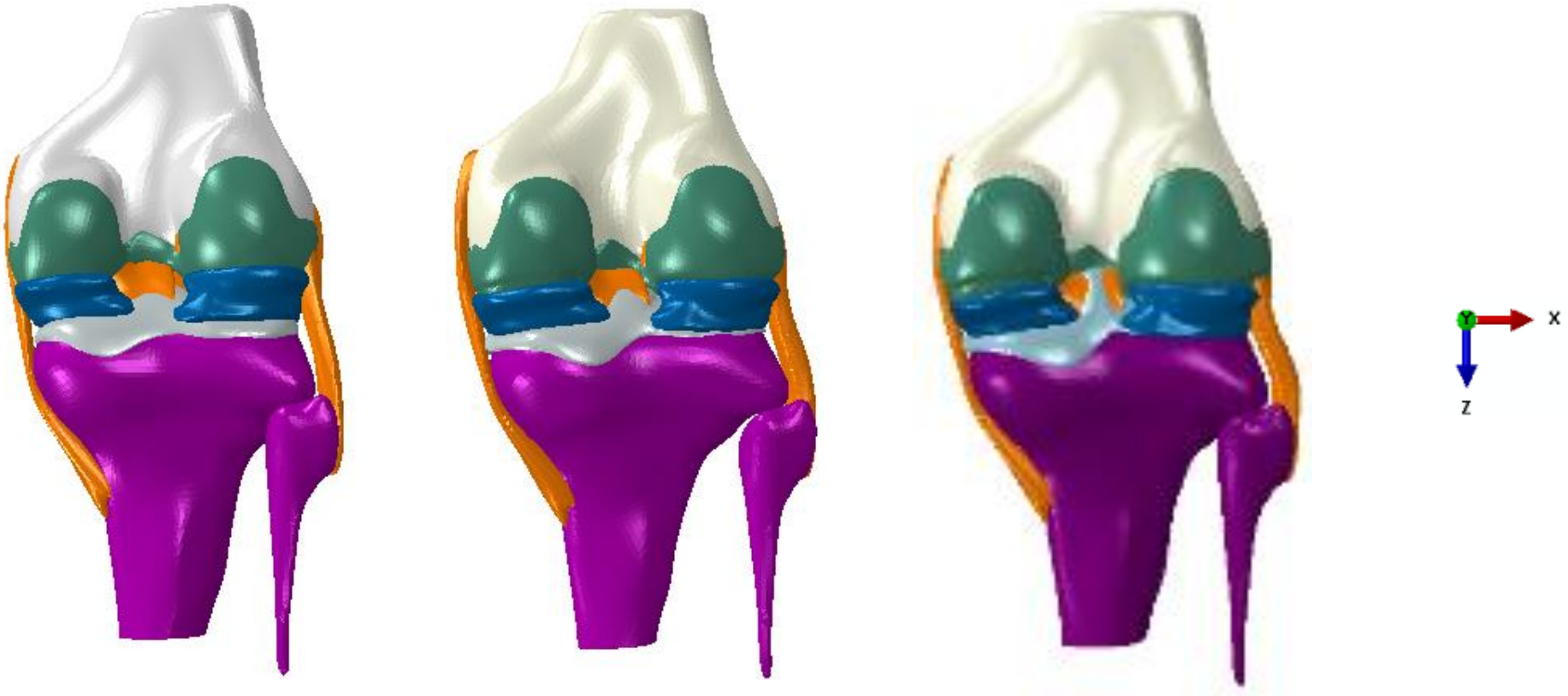

(a) Undeformed (b) Deformed (800 N load) (c) Deformed (1500 N load) (d) Axis

Figure 4-5 Undeformed and deformed models of 800 N and 1500 N loading

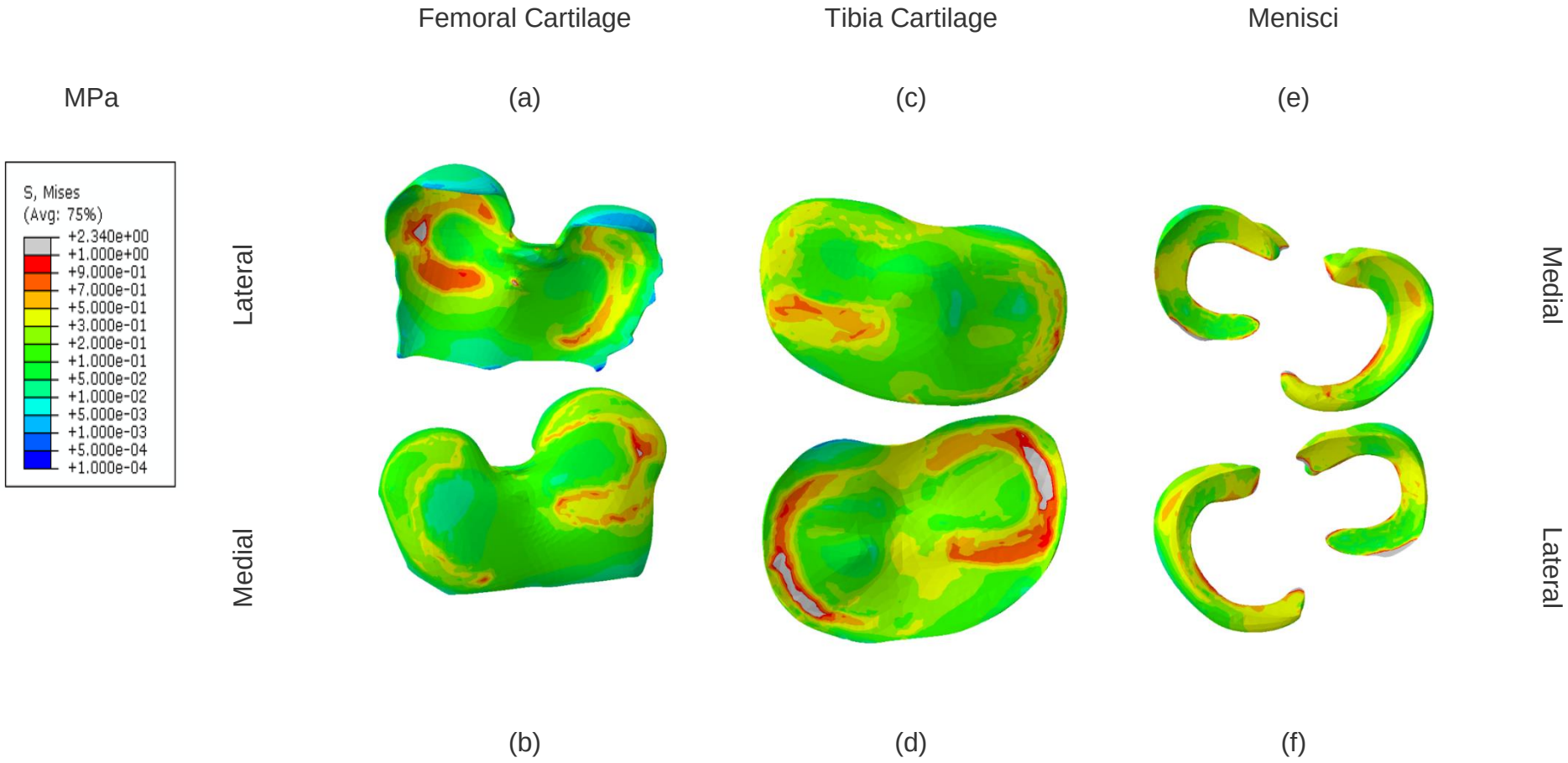

Figure 4-6 Simulated results of a healthy knee joint with 800 N loading (a) top view of femoral cartilage (b) bottom view of femoral cartilage (c) top view of tibia cartilage (d) bottom view of tibia cartilage (e) top view of menisci (f) bottom view of menisci

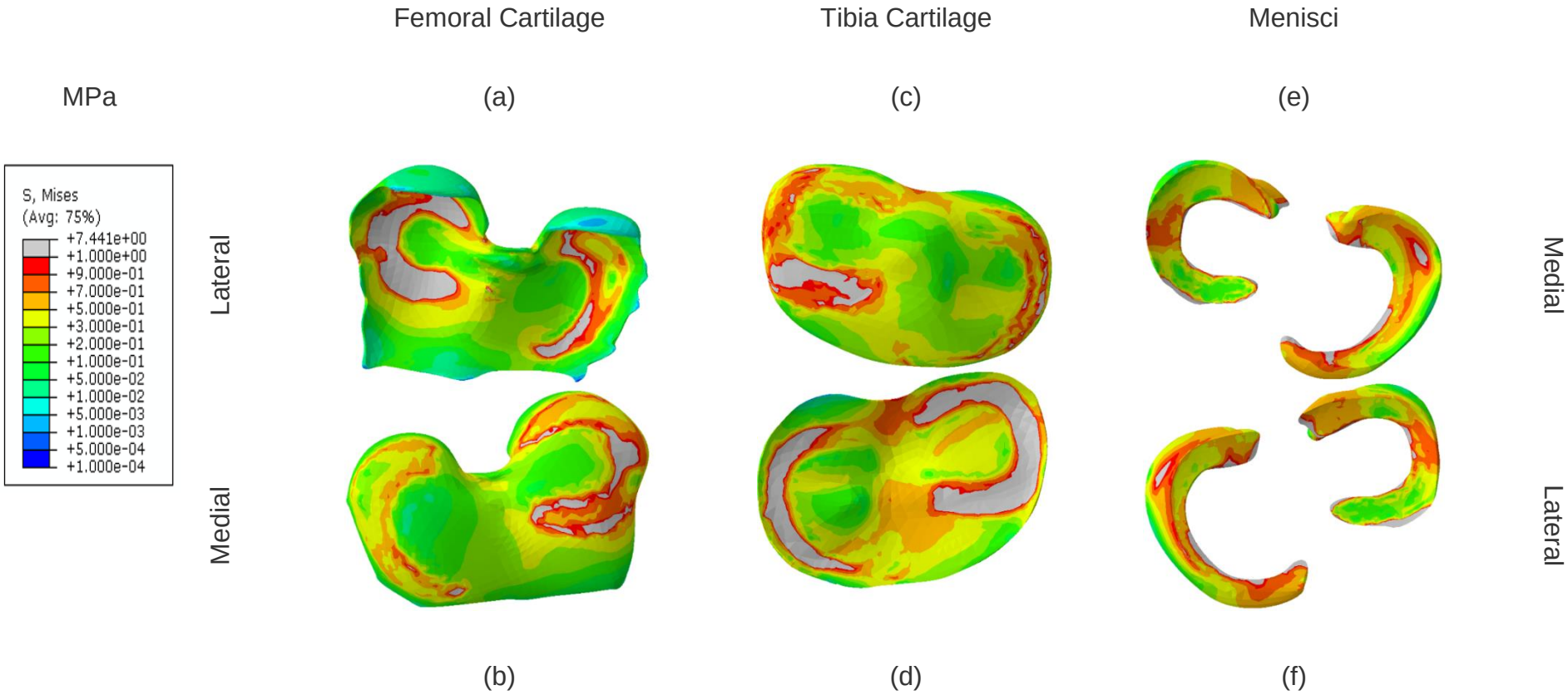

Figure 4-7 Simulated results of a healthy knee with 1500 N loading (a) top view of femoral cartilage (b) bottom view of femoral cartilage (c) top view of tibia cartilage (d) bottom view of tibia cartilage (e) top view of menisci (f) bottom view of meniscus

Comparison of the stress distribution pattern on the femoral cartilage presented in Cartana et al. (2013) and the results of this research clearly shows that the maximum stress distribution occurs within the region where the cartilage is in contact with the meniscus. Another similarity is that the stress analyses in both studies show that maximum stress occurs on the medial compartment of the knee joint. Although Cartana et. al (2013) performed their analysis on the left knee, this research analysed the right knee. In addition, the size of the models of the two researches are different which may explain the slight differences between the results for the model of the healthy knee.

An 800 N load is applied to the femur based on the experimental data. The distal base of the tibia and the rotation of varus-valgus and flexion-extension are fixed. The contact properties applied in the model are taken from Cartana et. al (2013).

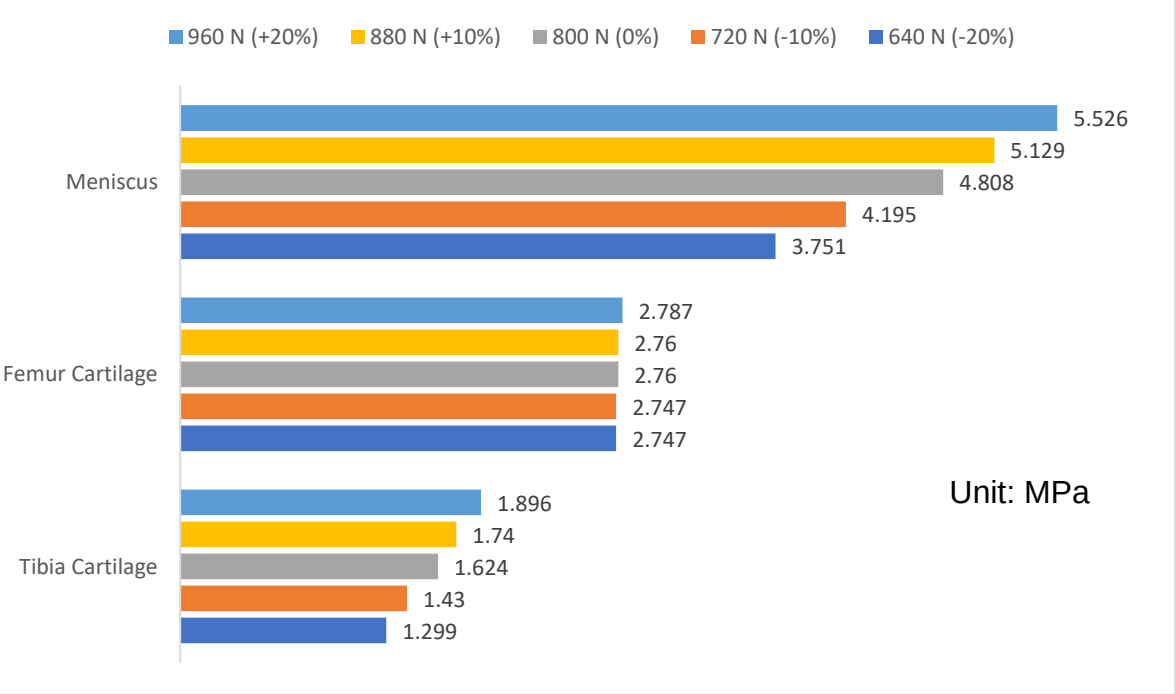

Figure 4-8 Sensitivity of Loading

The results of sensitivity analyses of loading conditions are presented in Figure 4-8. These sensitivity analyses have been done by varying the loading by ±20% with an interval of 10% and comparing each result against the result of 800 N load.

On the femoral cartilage, decreasing the load by 10% and by 20% caused the maximum von Mises stress to decrease by 0.47% from the result with 800 N load. On the other hand, increasing the load by 10% caused no change in the maximum von Mises stress, while increasing the load by 20% resulted in an increase of 0.98% in the maximum von Mises stress compared with 800 N loading.

However, the results of sensitivity analysis of tibial cartilage showed differences from the result with 800 N load. With a decrease of 20% in loading, the maximum stress decreased by about 20%. Also, the maximum von Mises stress was reduced by 12% for a 10% reduction in load. However, increasing the load by 10% caused the maximum stress to increase by 7% from the result obtained with 800 N load. Also the maximum stress increased by 17% when the load was increased by 20%.

Moreover, in the analyses on the meniscus, decreasing the load by 20% caused the maximum stress to decrease by 22% from the result obtained with 800 N load, while decreasing the load by 10% caused the maximum stress to decrease by 13%. On the other hand, increasing the load by 10% increased the maximum stress by 6.7%. Also, the results showed an increase in maximum stress of 15% with 20% increase in load, compared with the result obtained with 800 N loading.

The results of the sensitivity analysis show that increasing or reducing the load does not have much effect on the femoral cartilage. On the other hand, tibial cartilage and meniscus are quite sensitive to changes in loading conditions.

4.3. Discussion

In this chapter, a 3D model of a healthy human knee joint was constructed and used successfully in finite element analysis. The model included all the relevant parts including bony structures (femur, tibia, fibular, and patella), articular cartilage, menisci (lateral and medial), relevant ligaments (ACL, PCL, MCL, and LCL) and patellar tendon. The components of the model were assigned the exact material properties that were mentioned in the previous research. Linear elastic material behaviour was assumed, and the material properties were assigned to the model (Cartana et al., 2013). Even though the patellar tendon was created in the 3D model, the focus within this research is on the main complex of the knee joint during standing and midstance. Thus, the patellar tendon will not be included in the finite element analyses.

To validate the model, it was assigned the same material properties as mentioned in Cartana et al. (2013). The model used in this study focused only on the joint, while in Cartana et al. (2013), the model contained the full length of the lower extremity. Another point of difference is that Cartana et al. (2013) used the left leg, while this research used right leg to analyse the stress within the joint.

The results of these studies show that the maximum stress distribution occurred on the medial region of the joint. The results that were measured on each component are close to the results presented in the literature, which is explained

earlier in the results section. Thus, it can be said that the results of these analyses are partially validated against the literature.

Even though, the loading that was used within the analysis was taken from the data collection gait analysis, parametric studies were done, i.e., sensitivity of loading.

Analysis of sensitivity of loading enabled evaluation of the stress distribution pattern on each component, and the maximum stress results have increase and decrease according to the change in load. Figure 4-8 clearly shows that increasing and decreasing the load does not affect the femoral cartilage. In contrast, the maximum stresses on the tibial cartilage and menisci change dramatically, varying within the range of loading values (±10 and ±20%).

In conclusion, these sensitivity studies show that the femoral cartilage is not sensitive to any changes that have been done to the model. The tibial cartilage is slightly sensitive to the changes in boundary conditions, whereas the menisci are very sensitive to any changes that have been done to the model.

5. Finite Element Analysis on Osteoarthritis

5.1. Introduction

As mentioned in Chapter 2, section 2.3, OA is a disease that affects the joint and cartilage of the patients. The detail of symptom and the age range which has the risk of being affected by this disease was explained in section 2.2. Figure 5-1 shows a difference between a healthy knee joint and an OA affected knee joint.

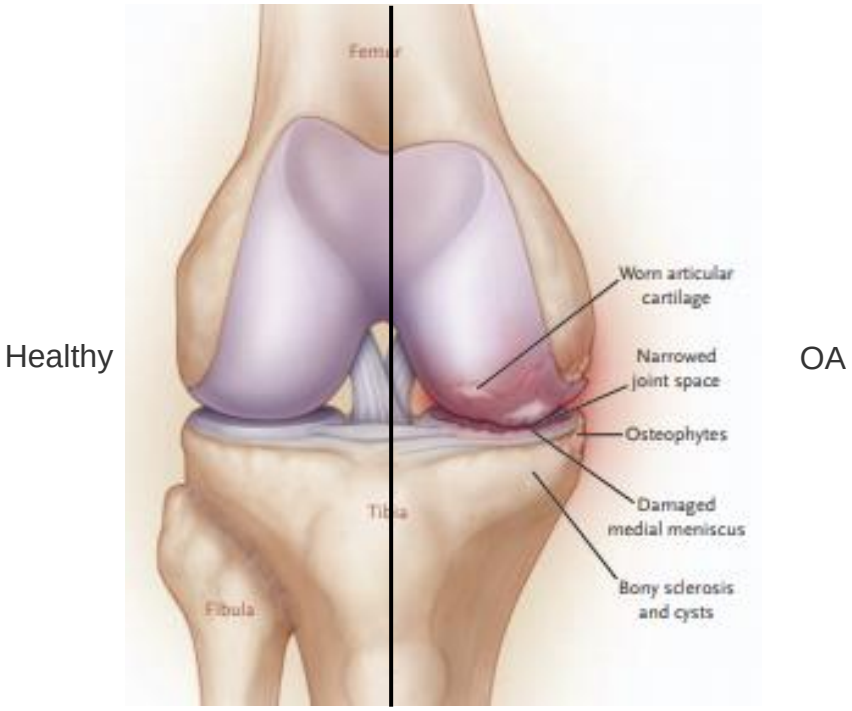

Figure 5-1 A healthy knee joint and OA affected knee joint (Felson, 2006)

5.2. Finite Element Simulation of Knee OA

In most cases, OA occurs due to the thinning of the cartilage (Nha et al., 2013; Mootanah et al., 2014), and it is most common on the medial side of the joint leading to valgus even though there is a possibility that OA can occur in the lateral zone leading to varus (Nha et al., 2013).The literature gives no information on how to design a degenerative outline of OA disease in finite element analysis.

Some research indicates that the material properties of cartilage and meniscus would be reduced by half (Cartana et. al, 2013; Tarniţă et. al 2014). In OA patients, the material properties of cartilage and menisci are certainly different from those in the healthy subjects. Table 5-1 shows the typical material properties of an OA knee (Cartana et. al, 2013; Tarniţă et. al, 2014).

Table 5-1 Osteoarthritis material properties

Geometry	Young's Modulus [MPa]	Poisson's Ratio
Femur	18600	0.3
Tibia	12500	0.3
Cartilages	*6*	*0.49*
Meniscus	*29.5*	*0.49*
Ligaments	10	0.49

In the development of the finite element, model for the OA knee, as the model was changed, and the thickness of the cartilage was reduced, a finer mesh was used for both cartilage and meniscus. Thus, the number of elements was increased (see Table 5-2).

Table 5-2 Element type and number of elements for OA model

Part	Element Type	Number of Element
Cartilages	Quadratic Tetrahedral	35129
Menisci	Quadratic Tetrahedral	15383

5.2.1. The Analysis of an OA Material Properties on a Healthy Knee Model

As mentioned above, finite element analysis of Osteoarthritis has rarely been done. In this section, a stress analysis of an OA knee will be carried out using OA material properties (Table 5-1) on the healthy knee model that was developed in the present thesis. The thickness of the cartilage remains the same as the healthy knee model (see Figure 4-1). The boundary conditions of this model are set to be the same as in the validated model with 800 N loading. This is to compare the stress distribution in the OA model against the stress distribution in the healthy model.

The maximum von Mises stresses that was measured on femur cartilage, tibia cartilage and menisci of 1.446 MPa, 1.109 MPa and 3.391 MPa respectively. The simulated results are presented in

Given these results, the next analysis is created to compares more results to find the most accurate simulation to represent the OA finite element analysis allowing comparison with the healthy knee model. The results of stress distribution are presented in Figure 5-2.

From the simulated results it can be seen that in the OA knee the stress distribution is reduced by half from the validated healthy knee which is not reasonable. According to the relationship between stress and strain, the stress varies with Young's modulus and strain. Also, stress varied with force and surface area; thus, Young's modulus affects stress.

Since the material properties of OA have been reduced by half but the force and surface area remain the same, stress should have increased. The results presented in Table 5-3 showed that the stresses in this model have decreased.

Table 5-3 The comparison of the maximum von Mises stress result between OA material properties on healthy knee model and healthy knee results, including percentage differences

Components	OA material on healthy knee model (MPa)	Healthy knee (MPa)	Different (%)
Femur cartilage	1.446	2.76	-47.61
Tibia cartilage	1.109	1.624	-31.71
Menisci	3.391	4.808	-29.47

With these results presented, the next analysis compares more results to find the most accurate simulation to represent OA in finite element analysis.

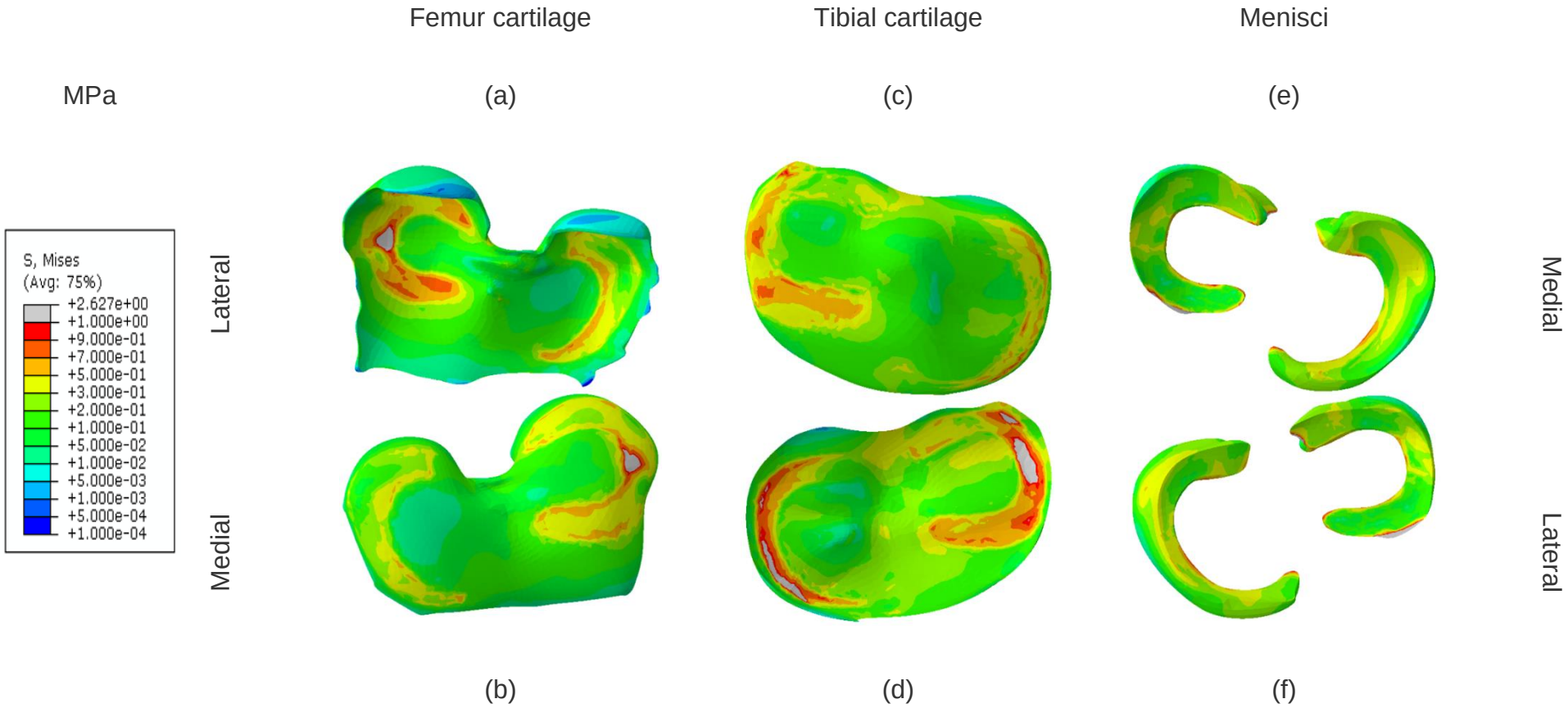

Figure 5-2 Simulated result of an OA knee material property on the healthy knee model with 800 N loading (a) top view of femoral cartilage (b) bottom view of femoral cartilage (c) top view of tibia cartilage (d) bottom view of tibia cartilage (e) top view of menisci (f) bottom view of meniscus

5.2.2. The analysis of a Healthy Knee Material properties on an OA Model

In the previous analysis, the result that were achieved were not accurate and did not agree with the theory. In this section, the analysis will be done on an OA model, in which the thickness of cartilage, both femur and tibia, has been thinned out by half. This has been done to replicate the symptom of the disease (Arthritis Research UK, 2013; Cartana et al, 2013). In this simulation, the results of maximum von Mises stress that were measured were 2.584 MPa, 2.67 MPa and 5.783 MPa on femoral cartilage, tibial cartilage and menisci respectively. The simulated stress distribution is presented in Figure 5-3 and a summary of the results is presented in Table 5-4.

Table 5-4 Simulated result of an OA model with healthy knee material property comparing against the healthy knee, including percentage differences

Parts	Healthy knee material on an OA model (MPa)	Healthy knee (MPa)	Percentage Difference (%)
Femoral cartilage	2.584	2.76	-6.38
Tibial cartilage	2.672	1.624	64.53
Menisci	5.783	4.808	20.28

In these results, the stress distribution in this analysis has increased; this is not the same as the result from the healthy knee joint. The maximum change is in the tibia cartilage in which the maximum stress has increased by 65%.

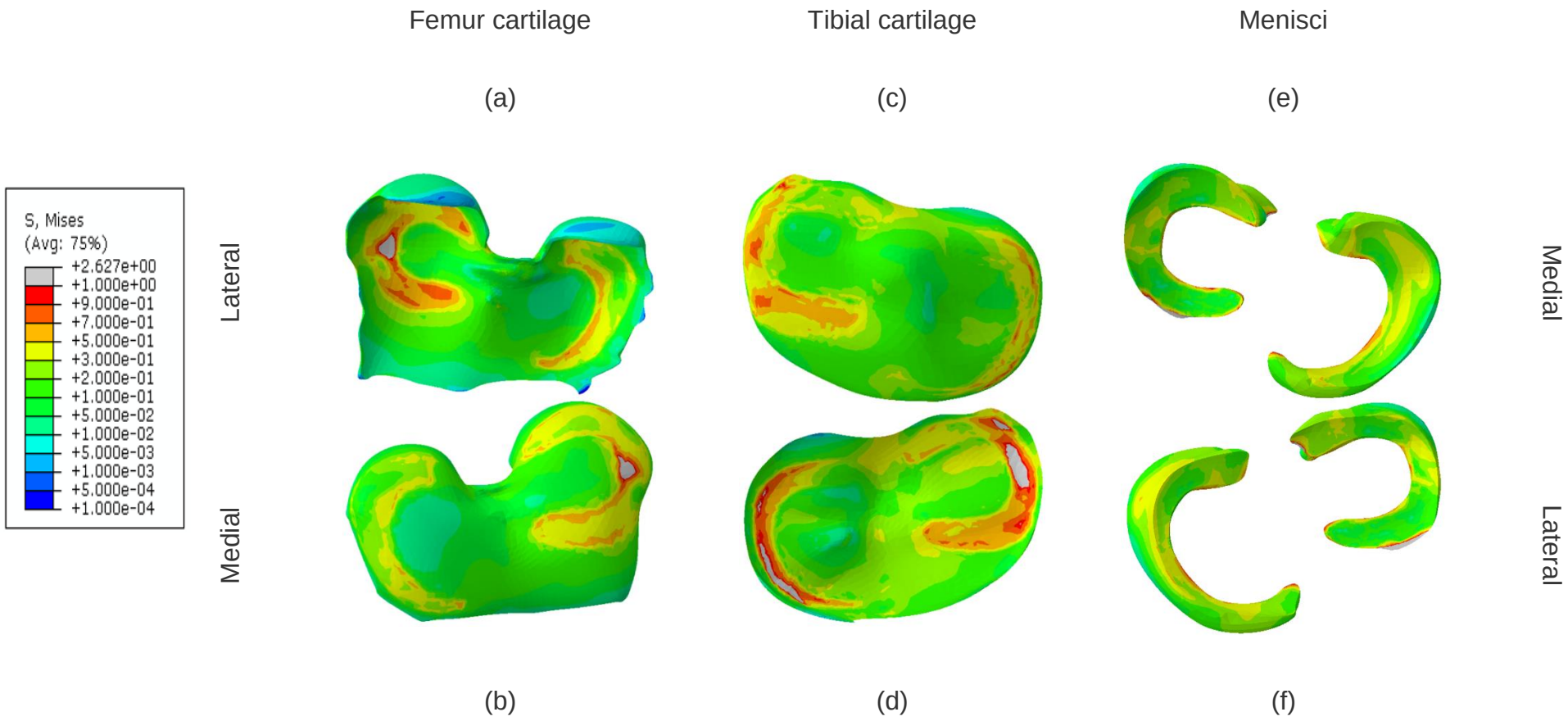

Figure 5-3 Simulated result of a healthy knee property on an OA Model with 800 Newton Loading (a) top view of femoral cartilage (b) A Bottom view of femoral cartilage (c) Top view of tibia cartilage (d) A Bottom view of tibia cartilage (e) Top view of menisci (f) A bottom view of meniscus

In these results, there is an improvement and it is assumed to be on the right track to find the accurate finite element model for Osteoarthritis. For further analysis, the combination of the two models, OA material property with the OA model will be considered.

5.2.3. Investigating the effects of OA Material Property on its Behaviour

The previous analysis shows improvement in the stress distribution of the model. As mentioned above, the combination of using OA material property with the OA model is taken into consideration. The model that will be used in this analysis is the same as the previous analysis and the material property of OA is in Table 5-1.

Figure 5-5 shows the deformation of an OA model with a 50% reduction of material properties and thinning of the cartilage by half. The cartilage has collapsed, and the menisci are torn in the posterior-lateral side of the joint. The simulated result of an OA with 800 N loading is presented in Figure 5-4.

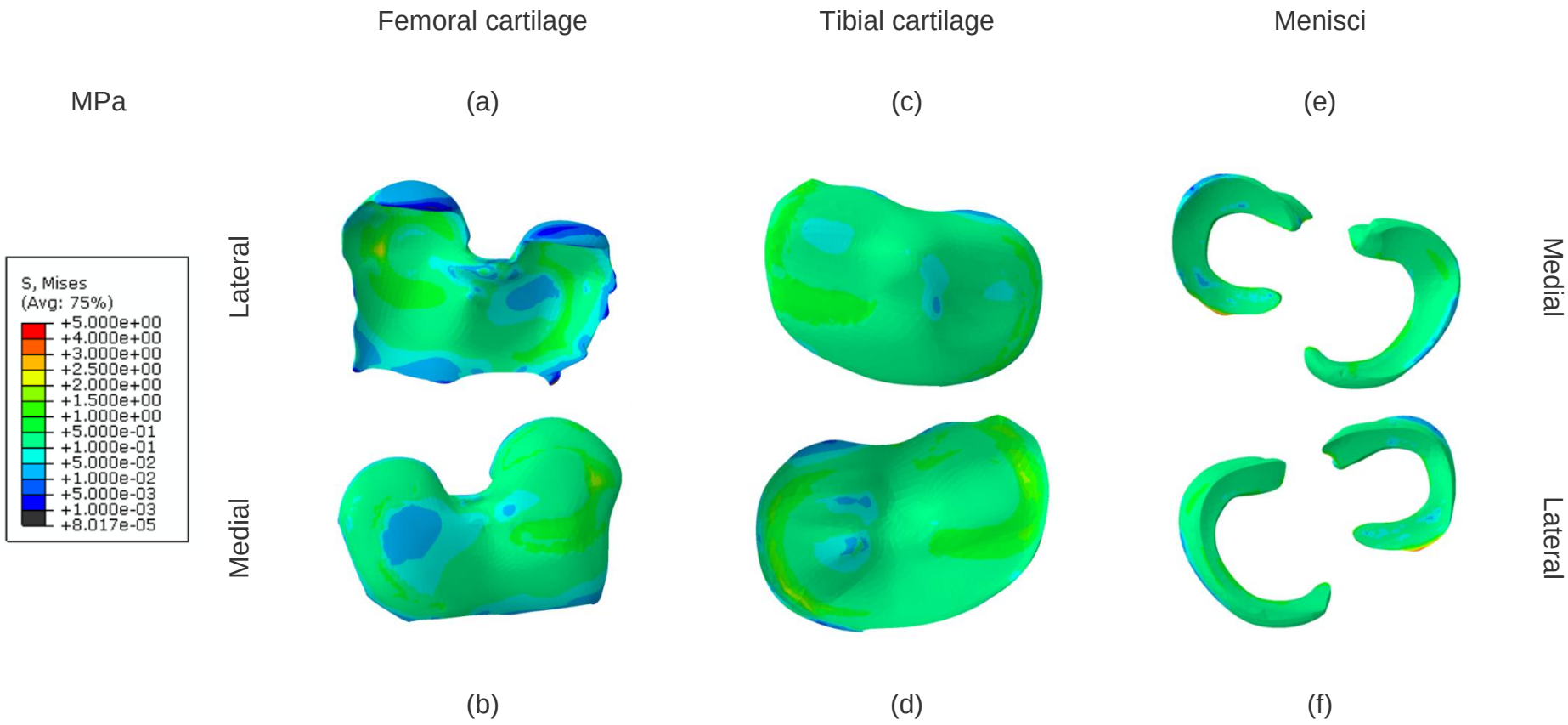

Figure 5-4 Simulated result of OA material properties on healthy knee model with 800 Newton Loading (a) top view of femoral cartilage (b) A Bottom view of femoral cartilage (c) Top view of tibia cartilage (d) A Bottom view of tibia cartilage (e) Top view of menisci (f) A bottom view of meniscus

The maximum von Mises stress values that were measure on the model are 2.571 MPa, 3.925 MPa and 4.177 MPa (femoral cartilage, tibial cartilage, and menisci respectively. The maximum stress that was measured on the femoral cartilage was taken at the lateral-posterior while on the tibial cartilage, the measurement was taken at medial-anterior for the menisci it was taken at the lateral-posterior side of the joint. The summarized results are presented in Table 5-5, which also compares the results of this analysis against the validated healthy knee result including percentage differences.

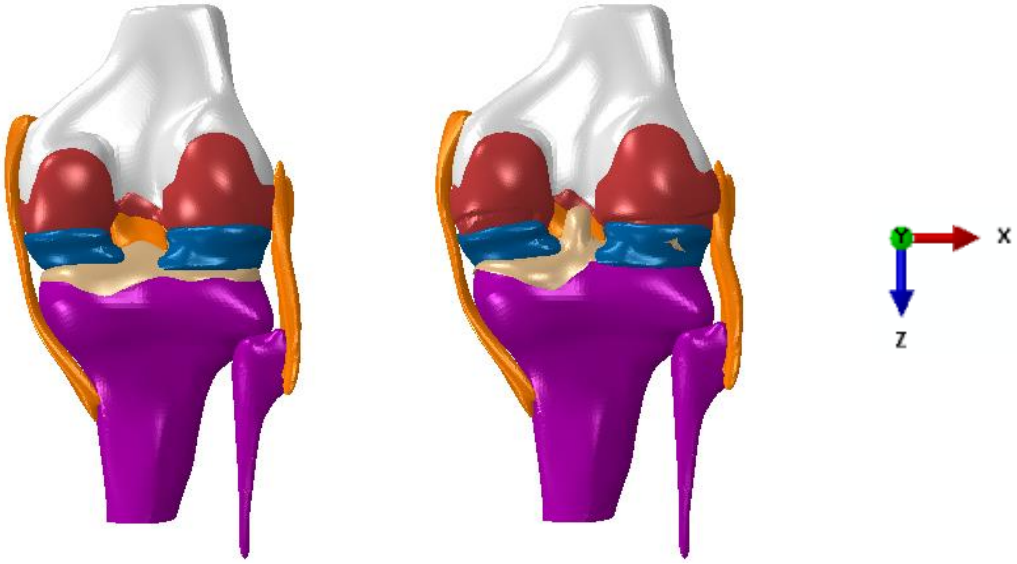

(a) Undeformed OA model (b) Deformation of OA model with 800 N Load (c) Axes

Figure 5-5 Undeformed and deformed model of OA knee

Table 5-5 Maximum von Mises stress results ~~of an OA material property on~~for the OA model compared against the validated healthy knee result, including percentage difference

Parts	The OA knee material on an OA model (MPa)	Healthy knee (MPa)	Percentage difference (%)
Femur cartilage	2.571	2.76	-6.85
Tibia cartilage	3.925	1.624	141.69
Menisci	4.177	4.808	-13.12

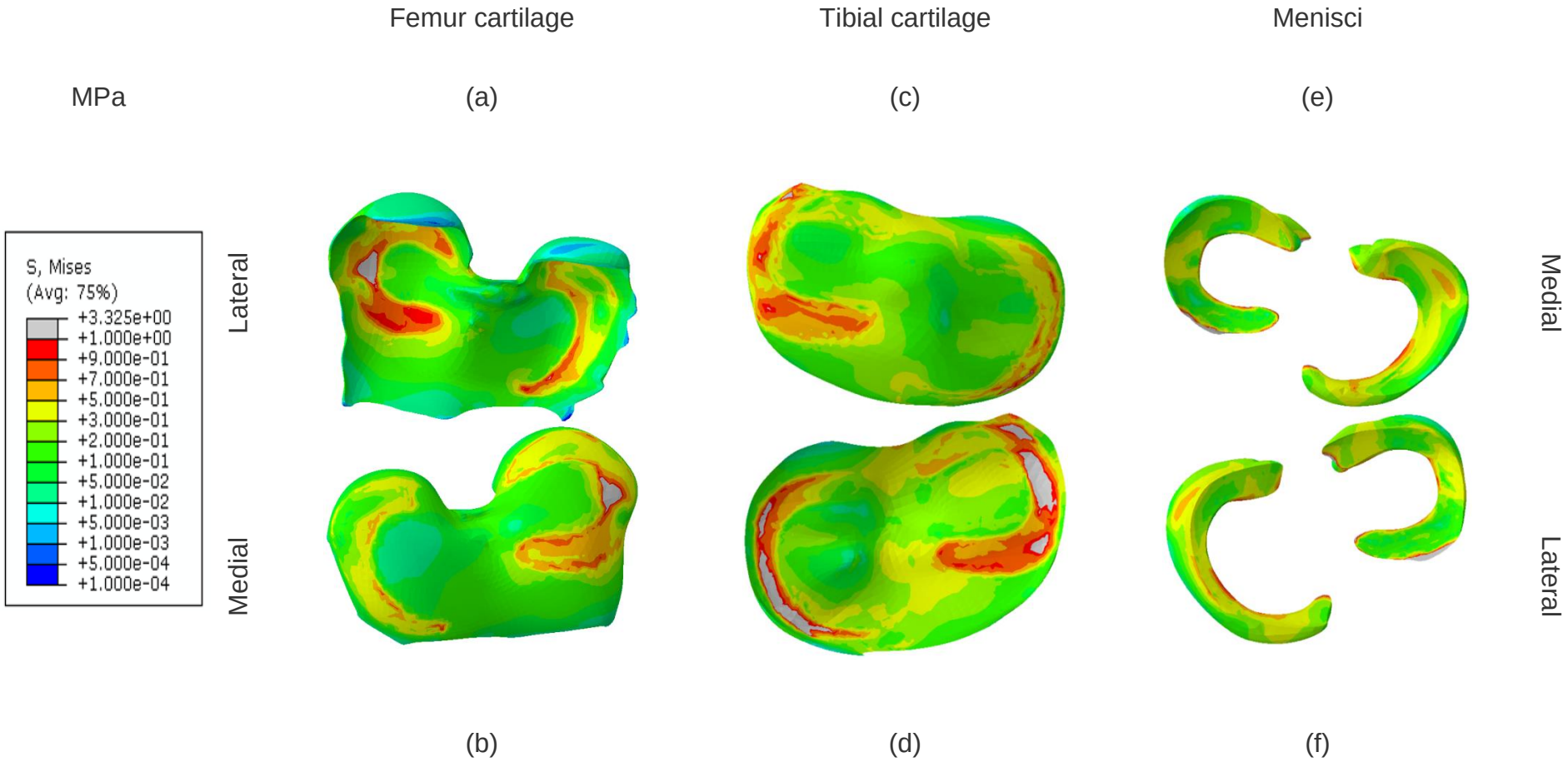

Figure 5-6 Simulate result of an OA knee with 800 N loading (a) top view of femoral cartilage (b) A Bottom view of femoral cartilage (c) Top view of tibia cartilage (d) A Bottom view of tibia cartilage (e) Top view of menisci (f) A bottom view of menisci

5.3. Discussion

In theory, stress will vary with the applied force for the given load and the surface area; the smaller the surface area, the higher the stress is. Osteoarthritis is a joint disease which degenerates the soft tissue within the joint. With this degeneration of the soft tissue, the surface area of the cartilage is decreased, so the stress in the joint should be increased.

In this chapter, the results of stress analysis were compared for three cases: (i) OA knee represented by change in material properties of cartilage on a healthy knee joint model; (ii) OA knee represented by reduction in the thickness of cartilage and using the material properties of a healthy knee; and (iii) OA knee represented by both reduction in the thickness of cartilage and change in the material properties of cartilage. All analyses were done under a compressive load of 800 N and three simulations were carried out. The first simulation was done on the validated healthy knee model with osteoarthritis material properties. This simulation was done to examine the effect of the change in the material properties on the stress distribution in the knee joint. The results showed a reduction in stress compared with the validated healthy model. The difference in stress in each component of the joint was high with a reduction of maximum in stress of 47%.

The second simulation was carried out to examine the effects of the reduction in thickness of the cartilage (i.e. wearing away of the cartilage) on the behaviour of the OA knee joint. The results have shown that the stresses increased compared to the healthy knee model. The maximum stress increase was 65%, in the tibia cartilage.

The third simulation was set up to study the combined effects of OA in terms of the change in material properties as well as the change in thickness of the cartilage. The results showed that the stresses increased compared to those in the healthy knee with a maximum percentage increase more than 100% found at the tibial cartilage. The summary of the results of the three simulations compared against one another and against the validated healthy knee model is shown in Table 5-6.

Table 5-6 Comparison of the Maximum von Mises Stresses in Healthy Knee and OA Knee Models

Part	Healthy (MPa)	Result from 5.2.1 (MPa)	Result from 5.2.2 (MPa)	Result from 5.2.3 (MPa)
Femur cartilage	2.76	1.446	2.584	2.571
Tibia cartilage	1.624	1.109	2.672	3.925
Menisci	4.808	3.391	5.783	4.177

From these analyses it is observed that decreasing the Young's modulus of articular cartilage and menisci and increasing the Poisson's ratio of the cartilage leads to substantial increase in the maximum von Mises stress within the cartilage and menisci. These simulated results demonstrated that the maximum von Mises stress is sensitive to the change in material properties and thickness of the cartilage. It can be concluded that, to adequately simulate the cartilage degenerated due to the disease, the finite element model for OA should have two

main components the material properties and the change in thickness of the cartilage.

6. Finite Element Modelling of Varus Deformations in Osteoarthritis

6.1. Simulation of Varus Condition

As mentioned in Chapter 1, one of the objectives of this thesis is to analyse and replicate varus and valgus condition using the finite element method. In previous studies, varus and valgus conditions were modelled in finite element analysis by setting the angle to the model during the initial assembly. This method can be used if the mechanical axis can be identified. In the present thesis, however, the model focuses only on the knee joint, and thus does not contain the full length of the lower extremity. Due to the length of the model, the difference in angle between the initial mechanical and deformed mechanical cannot be specified. One solution to replicate a varus-valgus analysis is to use basic knowledge of engineering i.e. static analysis and moment of force.

The analysis in this thesis is based on a fully extended knee, both midstance and standing. In the modelling of varus and valgus condition in this section, all rotations axes of flexion-extension and internal-external will be ignored and the analysis will focus on the rotation over an axis that will produce varus or valgus conditions.

In simulating varus and valgus conditions, the change in the angle of the model is considered based on the literature. However, due to the uncertain and unspecified condition of the axis of the anatomic and mechanical axes of the present model, moment of force is introduced to replicate the change in angle in the varus and valgus conditions. This method is used in order to prevent inaccurate results and to avoid changing of the validated model. The moment of

force can be applied on either clockwise or anti-clockwise relative to the Y axis depending on which simulation is planned, varus or valgus.

In this research section, the validated healthy knee joint model is used to simulate varus conditions with the loading of 800 N. The boundary conditions are set the same as in the validated model.

Equation 6-1 present the relationship between moments, M of a force F that is applied with eccentricity (e); F in this case is the weight of human body.

$$\boldsymbol{M = Fe} \qquad \text{Equation 6-1}$$

The eccentricity can be determined as:

$$\boldsymbol{e = \tan\theta \times x} \qquad \text{Equation 6-2}$$

Where x is the length of the femur and θ is the misalignment angle. The average length of a male femur is 480 millimetre (Naderi-pour, 2010). In Equation 6-2

$$e = \tan 7.25 \times 480$$

$$e \cong 55\ mm$$

Substituting the estimated value of e in Equation 6-1 yields;

$$M = 800 \times 55$$

$$M = 44000\ Nmm$$

As mentioned in Chapter 5, OA mostly occurs in the medial region of the knee joint. The simulations have been done based on a healthy knee model using the material properties of the healthy knee (see Table 4-1). Three different

simulations were carried out for 3 varus cases of 3.8° varus; misalignment angles of 5.18° and 7.25°; the deformation results are shown in Figure 6-1.

As expected, the deformation patterns of the increasing misalignments show progressive change from the lateral side to the medial as compared with the healthy model (see Figure 6-2).

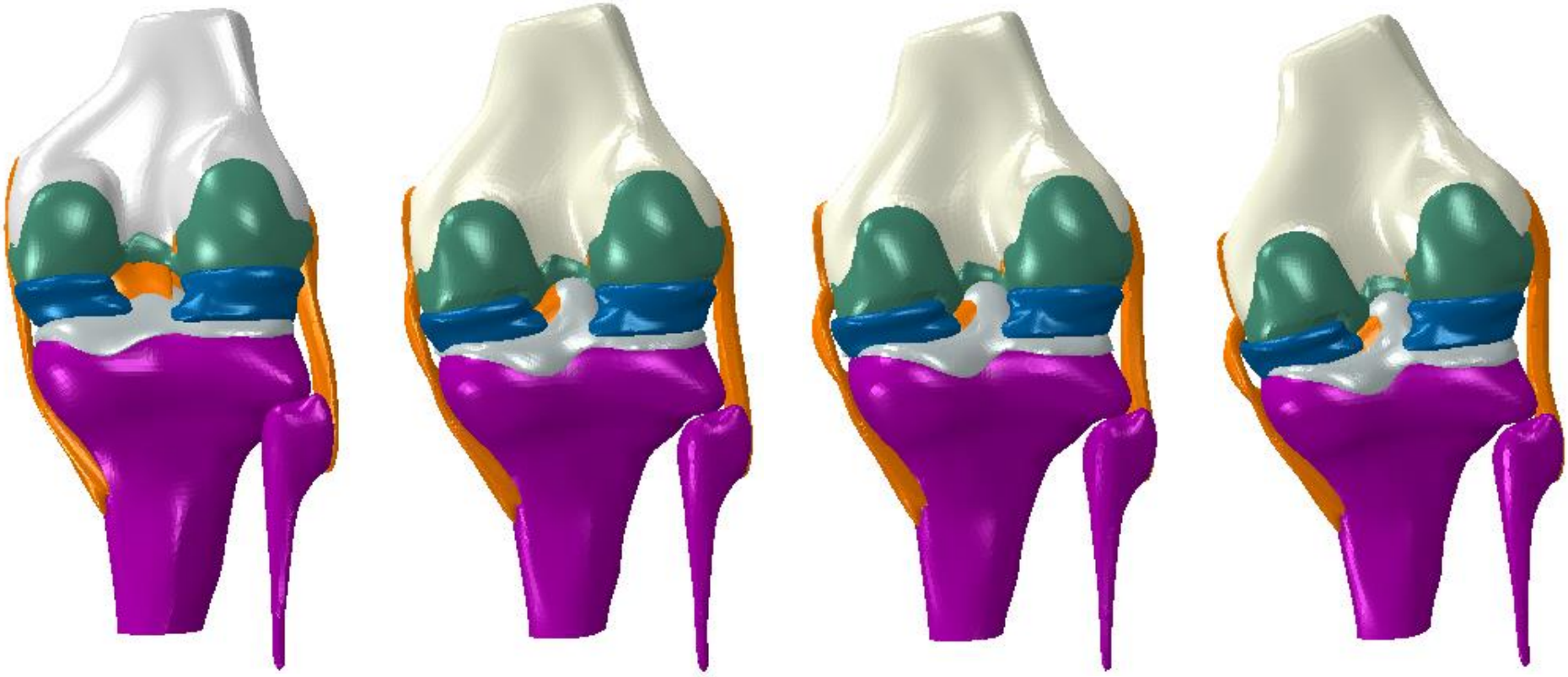

(a) Undeformed

(b) Deformed (3.8° Varus or moment of 24600 Nmm)

(c) deformed (5.18° Varus or moment of 34800 Nmm)

(d) deformed (7.25° Varus or moment of 44000 Nmm)

Figure 6-1 Undeformed and deformed joint for various varus conditions

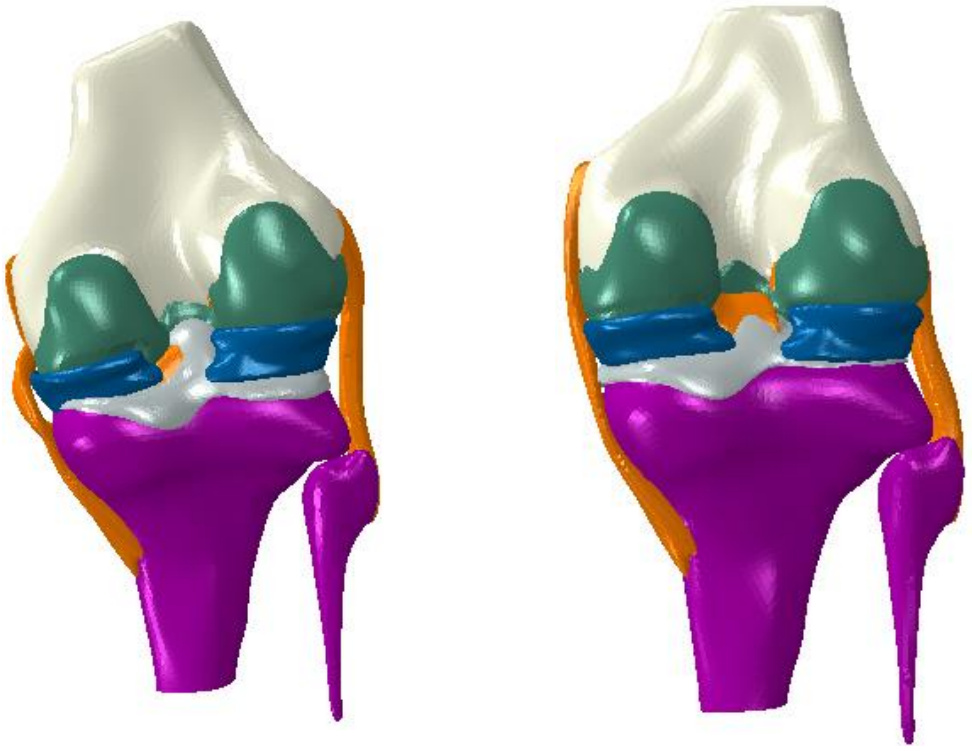

(a) (b)

Figure 6-2 Comparison (at 7 times magnification) between (a) the deformed models for varus at 7.25° and (b) healthy knee.

The distribution of the von Mises stress for varus angles of 3.8, 5.18°, and 7.25° are shown in Figure 6-3, Figure 6-4 and Figure 6-5 respectively. The results show that in all three cases, the maximum stress occurred on the medial side of the knee joint. The maximum von Mises stress that were predicted by the model with 44000Nmm are 4.144 MPa, 4.768 MPa and 4.949 MPa on the femoral cartilage, tibial cartilage and meniscus respectively. For 34800 Nmm., the maximum von Mises stress were 3.275 MPa, 4.094 MPa and 3.865 MPa in the femoral cartilage, tibial cartilage and meniscus respectively. For 25600 Nmm., the maximum von Mises stress measured on the model were 2.433 MPa, 3.393 MPa and 3.012

MPa in the femoral cartilage, tibial cartilage and meniscus respectively. A summary of these results is presented in Table 6-1.

Table 6-1 Result summary of results for various varus angles and the healthy knee joint

	Maximum von Mises stress			
Part	Healthy knee joint (MPa)	3.8° varus (MPa)	5.18° varus (MPa)	7.25° varus (MPa)
Femur cartilage	2.76	2.433	3.275	4.144
Tibia cartilage	1.624	3.393	4.094	4.768
Menisci	4.808	3.012	3.865	4.949

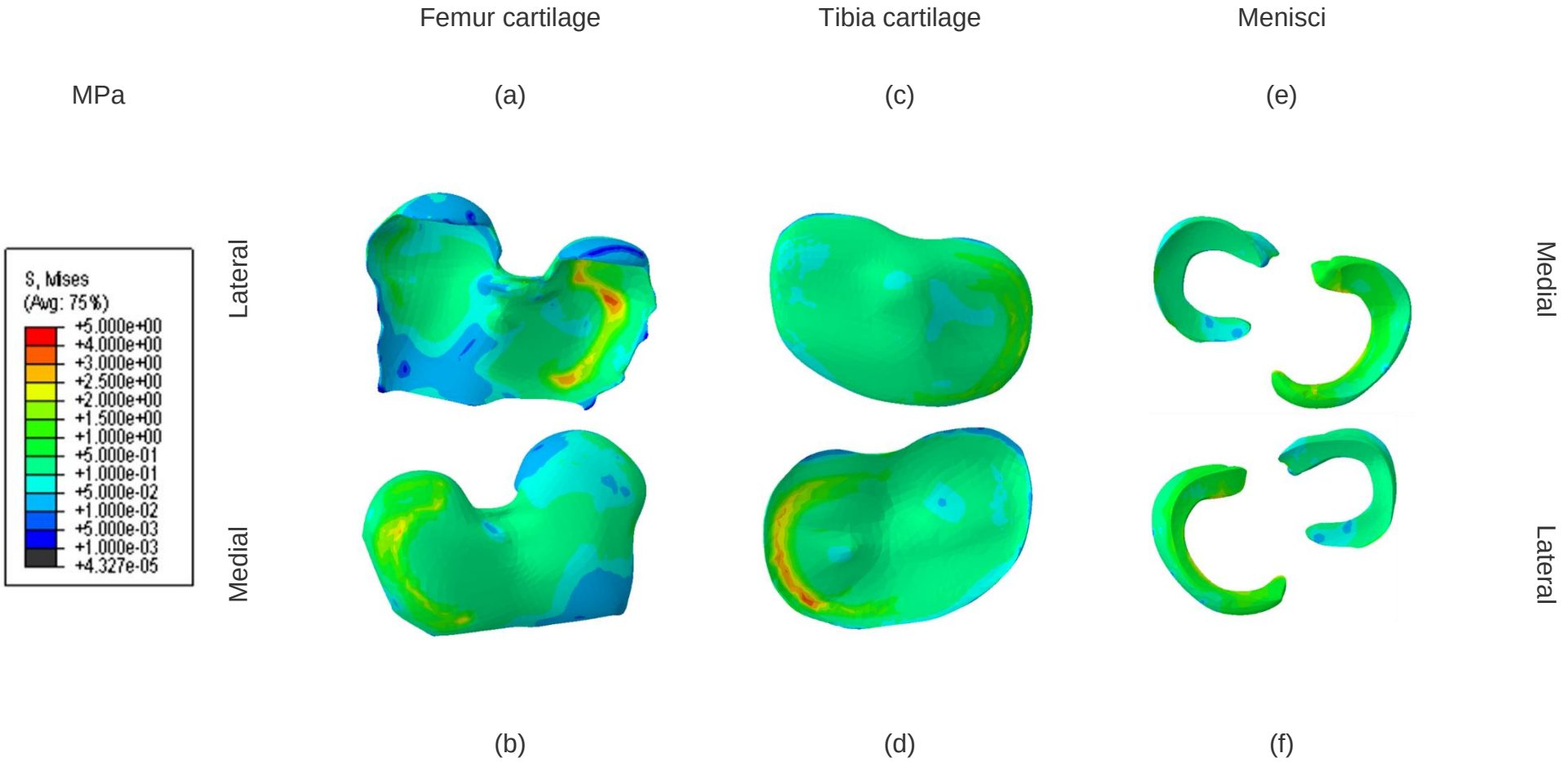

Figure 6-3 Distribution of von Mises stress for 3.8° or 24600 Nmm varus (a) top view of femoral cartilage (b) bottom view of femoral cartilage (c) top view of tibia cartilage (d) bottom view of tibia cartilage (e) top view of menisci (f) bottom view of meniscus

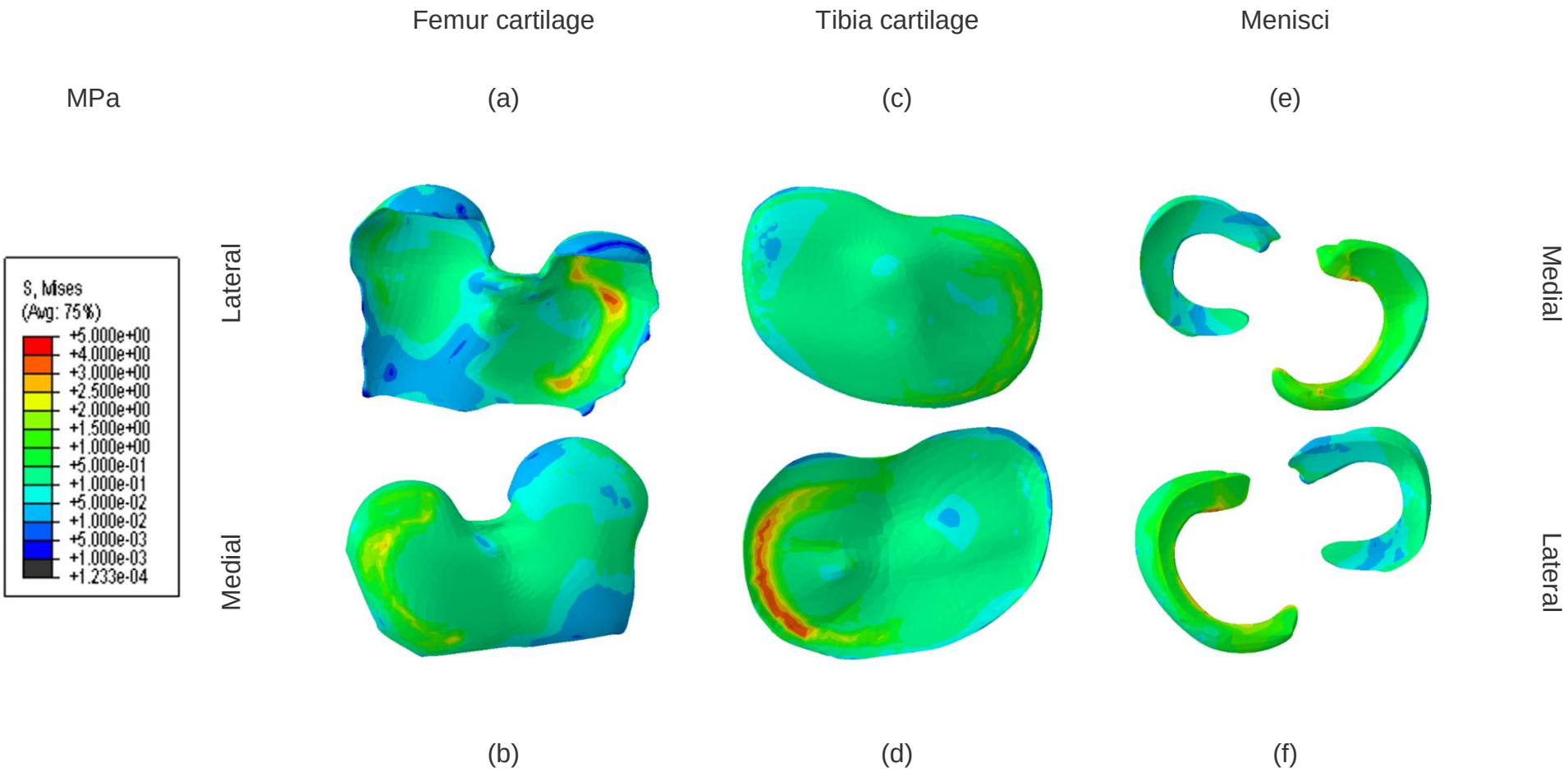

Figure 6-4 Distribution of von Mises stress for 5.18° or 34800 Nmm Varus (a) top view of femoral cartilage (b) bottom view of femoral cartilage (c) top view of tibia cartilage (d) bottom view of tibia cartilage (e) top view of menisci (f) bottom view of meniscus

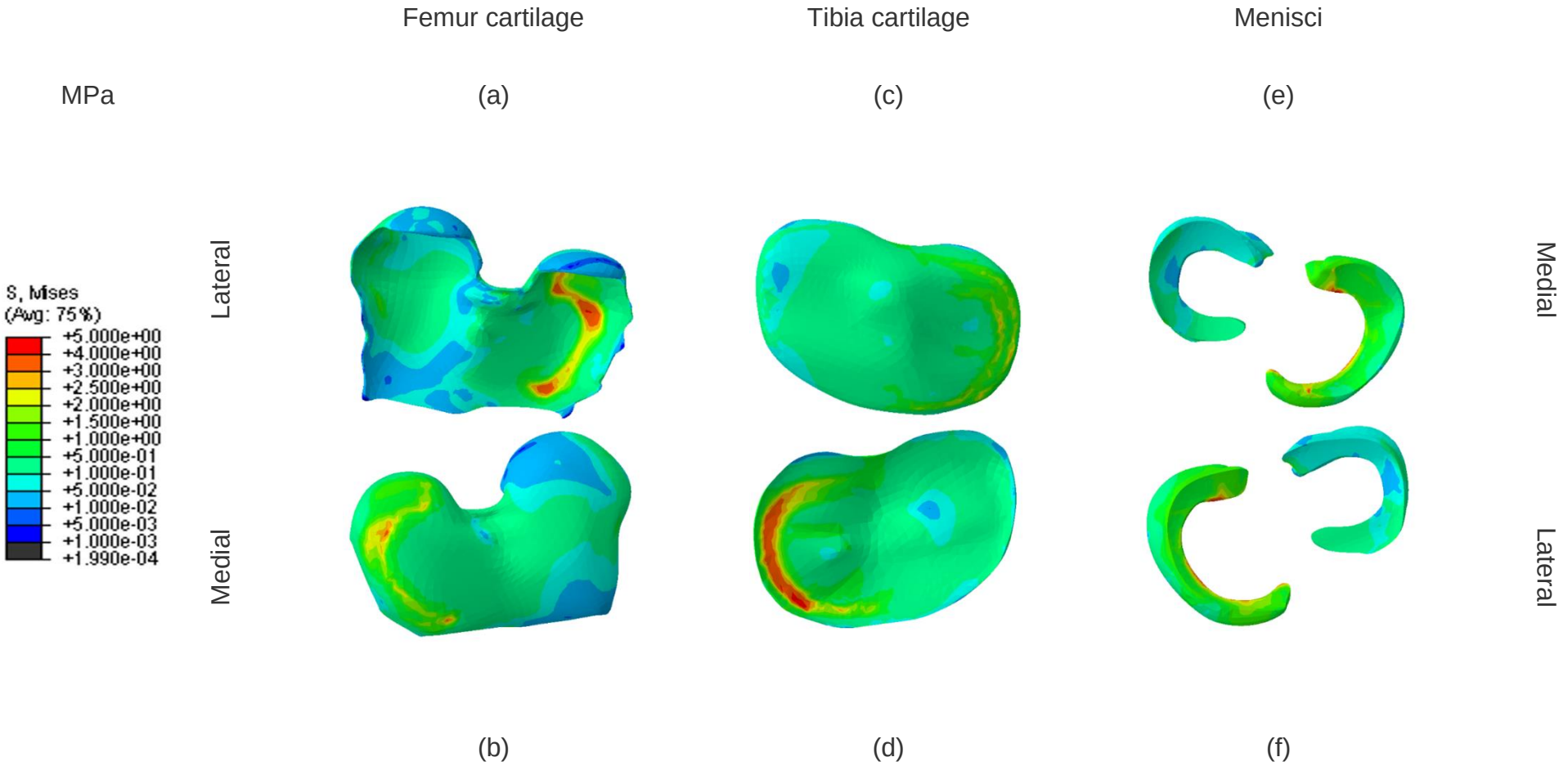

Figure 6-5 Distribution of von Mises stress for 7.25° or 44000Nmm Varus (a) top view of femoral cartilage (b) bottom view of femoral cartilage (c) top view of tibia cartilage (d) bottom view of tibia cartilage (e) top view of menisci (f) bottom view of meniscus

Other than the maximum von Mises stress, the maximum contact pressure was also predicted from the simulation models (see Table 6-2).

Table 6-2 Maximum contact pressure of various angle changes in varus condition

		Maximum contact pressure (MPa)					
Angle (°)	Moment (Nmm)	Bone		Femur Cartilage	Tibia Cartilage	Menisci	
		Femur	Tibia			Medial	Lateral
3.8	24600	2.112	2.651	12.45	7.634	54.98	16.27
5.18	34800	2.773	3.195	15.48	9.667	73.37	16.13
7.25	44000	3.328	3.65	13.31	13.17	85.72	12.35

6.2. Discussion

Osteoarthritis commonly occurs in the medial region of the knee joint and leads to joint deformation forming a varus or valgus condition. From the numerical model results of the healthy knee, the most affected region is in lateral region. Thus, the varus torque is taken into consideration to provide the required results. One of the objectives of this thesis is to replicate varus and valgus conditions without changing the angle, instead a moment is applied to represent the varus or valgus condition.

Three simulations were carried out with different varus angles: 3.8°, 5.18° and 7.25°. The model that was used in these simulations was the healthy model with as loading of 800N. The boundary conditions and the parameters of the contact

relations remained the same as in the FE model of the healthy knee. An additional parameter that was used in the model was the varus torque which was assigned around y axis. The results of the simulations showed that the torque that was assigned in the model has successfully represented the varus condition. Figure 6-1 shows the deformed model of varus condition compared against the healthy knee model. The deformations of the two models were on the opposite regions of the knee joint. The maximum stress concentration changed from the lateral region (in the healthy knee) to the medial region (in the OA knee). A comparison of the results of the healthy knee model and the OA knee model with different degrees of varus angle are shown in Table 6-3 and Table 6-4.

The predicted maximum von Mises stress for the 3.8° varus angle or 24600 Nmm varus torque was 3.393 MPa on the tibia cartilage. Comparing the result against the healthy knee model, the difference was an increase by 109%. Comparing against the OA knee model, the difference was an increase of 14.5%.

The maximum von Mises stress for 7.25° varus angle or 44000 Nmm varus torque was 4.768 MPa in the tibial cartilage. The difference from the healthy knee model was also more than 100%. Comparing the maximum stress in the model with 44000 Nmm varus torque with that of the OA model, the difference is an increase of 19.4% in the tibia cartilage, an increase of 46.85% in femur cartilage and an increase of 16.92% at meniscus. The femur cartilage has the maximum change in stress, which means the maximum deformation is at the femoral cartilage.

The result presented in Table 6-1 showed that the load is gradually transferred from the femur cartilage to meniscus and to the tibia cartilage. As the stress increased on the region that was expected when moment was used, it can be

concluded that this method can successfully be utilized to simulate varus deformation using FE analysis without changing the angle of the model in the assembly stage.

Table 6-3 Comparison of the maximum von Mises stress of the healthy knee model and model with various varus angles

Part	Healthy knee joint	Result of 3.8° varus			Result of 5.18° varus			Result of 7.25° varus		
	stress (MPa)	stress (MPa)	Difference in stress from Healthy (MPa)	Percentage difference (%)	stress (MPa)	Difference in stress from Healthy (MPa)	Percentage difference (%)	stress (MPa)	Difference in stress from Healthy (MPa)	Percentage difference (%)
Femur cartilage	2.76	3.706	0.946	34.28	3.275	0.515	18.66	4.144	1.384	50.14
Tibia cartilage	1.624	3.393	1.769	108.93	4.094	2.47	152.09	4.768	3.144	193.6
Menisci	4.808	3.012	-1.796	-37.35	3.865	-0.943	-19.61	4.949	0.141	2.93

Table 6-4 Comparison of the maximum von Mises stresses of the OA knee model and model with various angle of varus angles

Part	OA knee joint	Result of 7.25° varus			Result of 5.18° varus			Result of 3.8° varus		
	Stress (MPa)	Stress (MPa)	Difference in stress from OA (MPa)	Percentage difference (%)	stress (MPa)	Difference in stress from OA (MPa)	Percentage difference (%)	stress (MPa)	Difference in stress from OA (MPa)	Percentage difference (%)
Femur cartilage	2.571	4.144	1.573	46.85	3.275	0.704	24.08	3.706	1.135	36.16
Tibia cartilage	3.925	4.768	0.843	19.4	4.094	0.169	4.21	3.393	0.532	14.54
Menisci	4.177	4.949	0.772	16.92	3.865	0.312	7.76	3.012	1.165	32.41

7. Conclusion and Future Work

7.1. Conclusion

The underlying objectives of this thesis were (1) to summarise the data available for finite element analysis, test methods, and material properties that were used in modelling of the human knee joint; and (2) to develop and analyse numerical models for a healthy knee, an OA knee and a varus knee using the finite element method. In order to generate the varus knee, varus torque was applied to the model to represent the varus effect. The first objective was reasonably accomplished, as this total knee-joint FE model represents a useful foundation for analysis of the behaviour of knee joint under various conditions. The second objective has also been accomplished, as the moment was successfully can be use in replicating varus and valgus angle instead changing the angle of the knee model during assembly.

The simulation results showed that the model geometry and boundary conditions utilized in this FE model are appropriate. Even though the simulation results of this study was validated to some extent against results from the literature for several reasons, i.e. the human knee joint is a complex joint which none is identical to another, the size of the model sample, the density of the bone sample, material properties, loading, boundary conditions, and assigned contacts used in different in each study.

After the healthy knee model was created, a model was developed for the OA knee. The results of the OA knee model were analysed and compared with those of the healthy knee model. The comparison of the results enabled understanding

of the stresses that occur within the joint due to the degeneration of the cartilage and meniscus. In the next step, a finite element model was developed to study the varus conditions.

In the healthy knee joint, the stress distribution has shown that the maximum stress within the joint occurs in the lateral compartment. The load is gradually transferred from the femoral cartilage to the menisci and then to the tibia cartilage. The maximum stress result that was measured on tibia cartilage is less than that on the femur cartilage, due to the shock absorbance and lubricating role of the meniscus within the knee joint. Thus, the stress that occurred in the tibia cartilage is less than that in the femoral cartilage.

On the other hand, in the creation of an osteoarthritis finite element model required significant trial and error. An assumption that was mentioned in the literature was taken into consideration, i.e. change in material property of cartilage and menisci (Cartana et al, 2013; Tarniţă et al, 2014). The change in material properties was assigned to the healthy knee model to study the change in stress occurring within the joint. However, the results first indicated that the stress that occurred within the joint is lesser than the validated result due to the change in material properties. A new finite element model was created with the knowledge of osteoarthritis disease that the cartilage is degenerating due to the disease, and modifications were made to the validated model. The cartilage of both femur and tibia were thinned out by half, and the material properties of the healthy knee were then assigned to the model to see the difference. The results presented in this analysis shown that the stress increased in all parts with an average increased in the stress of 26%. This increase is due to the thinned-out

cartilage. Given the results of this analysis, the next step was to combine the two analyses; change in material properties and modification of the model. The results show that the stress within the joint has increased compared against the healthy knee joint in all components, cartilages and menisci. The stress distribution and the deformation of the model show that the lateral compartment is the most affected region. The most affected part of this analysis is the cartilage.

Although the analysis has been performed for osteoarthritis, the disease can cause the deformation of varus or valgus. From the analyses, the most affected part of the joint is the lateral compartment which caused valgus. Previous study (Vincent et al., 2012) indicate that osteoarthritis most commonly occurs in the medial compartment. Thus, analysis of varus deformation was undertaken. From previous studies (Pollo et al., 2002; Yang et al., 2010; Sun et al., 2016), in creating varus or valgus, the initial knee joint model was set to a certain angle depending on the previous studies assumption. To create a varus or valgus angle the anatomical axis must be located (see Figure 1.4). In the present thesis, it was important to locate the anatomical axis, due to the size of the model sample, so basic engineering static analysis, (i.e. moment) was adapted for use in this research. To perform the analyses varus torque was set to the initial model along with the loading of 800 N. The moment was calculated using the fundamental equation of Newton's second law of motion. The results indicated that the stress distribution changed from the lateral compartment to the medial compartment as expected. The higher the angle, the larger the stress that occurred proving that, the higher the stress, the higher the chance of developing osteoarthritis.

In conclusion, this research has simplified an accurate three dimensional geometrically model of the human knee joint for studying tibiofemoral stress. It also, finalized a finite element model of osteoarthritis and resulted in creation of a model of varus and valgus effects, using a basic engineering static analysis, moment, rather than changing the angle on the initial model. This method is very beneficial because it can be used when unable to identify the anatomical axis.

7.2 Problems Faced

The simulations using the finite element method took too much time due to the complexity of the model and the large number of elements and nodes, occasionally becoming impractical for the time spent. Another problem was that the computer processing unit (CPU) that was used in this study was slow due to the complexity of the model and the ABAQUS program took a large capacity of memory to run each analysis. Thus, high computer processing unit (HCPU) could help with saving time. Another way would be to run the analysis on several computers. In this research, the researcher had requested to use the HPCU, but the problem that was faced was the program the researcher use was not installed on the HPCU system. Although the request had been made and was accomplished to have the program install on the system, the researcher had finished running every analysis by the time the technicians installed the program on the system.

7.3 Future Work

Despite the limitations, the FE model developed in this thesis produced positive results and proved that it could be used to compute different aspects of the behaviour of the healthy and OA knee joint. It provides a sound basis for static and dynamic analysis of the knee joint at different stages of the gait and using a more complex material model in the future. Another possible future development could be to use the model to identify more accurate material models and material properties for the cartilage and meniscus and other parts of the knee joint.

One point is that the actual knee has a more complicated composition than that considered in this thesis; it is common to simplify FE models, and the present thesis is no exception. For example, the synovial fluid surrounding in the knee compound, which has the ability to absorb and distribute the load, could be included. Moreover, muscles around the leg bones and the knee and their forces could be included in the model. The model could be further developed by using more accurate material and material properties such as the poroelastic model for the cartilage and menisci.

The models developed, and the results presented in this study can be further developed and used in future research for example for the development of appropriate knee braces for osteoarthritis, as osteoarthritis is worsened by weight or body forces through an affected joint. Although there is a wide range of devices that are available to help people with osteoarthritis in different joints, there have been very few trials to demonstrate their efficiency, and in particular little data exist to guide healthcare professionals regarding which patients would benefit most from these aids. For example, there are many knee braces available, but

there are very few well designed randomised controlled trials of their efficiency, and few suggestions for clinicians on which patient sub-groups might benefit from their use. Although there are knee braces for OA patients in the market, they are mostly custom-made which may take a long time to create one. This research could be very helpful in term of reducing the time in casting a brace for a knee OA patient, with or without varus or valgus condition.

References

Akrami, M., Qian, Z., Zou, Z., Howard, D., Nester, C. J. and Ren, L. (2018) 'Subject-specific finite element modelling of the human foot complex during walking: sensitivity analysis of material properties, boundary and loading conditions', *Biomechanics and Modeling in Mechanobiology*. Berlin/Heidelberg: Springer Berlin Heidelberg, 17(2), pp. 559–576. doi: 10.1007/s10237-017-0978-3.

Allard, P. (1997) *Three-Dimensional Analysis of Human Locomotion*. Wiley (International Society Biomechanics series). Available at: https://books.google.co.uk/books?id=Fs9qAAAAMAAJ.

Allet, L., Knols, R. H., Shirato, K. and de Bruin, E. D. (2010) 'Wearable Systems for Monitoring Mobility-Related Activities in Chronic Disease: A Systematic Review', *Sensors (Basel, Switzerland)*. Molecular Diversity Preservation International (MDPI), 10(10), pp. 9026–9052. doi: 10.3390/s101009026.

Angulo, R. M. and Dapena, J. (1992) 'Comparison of Film and Video Techniques for Estimating Three-Dimensional Coordinates within a Large Field', *International Journal of Sport Biomechanics*, 8(2), pp. 145–151. doi: 10.1123/ijsb.8.2.145.

Antunes, P. J., Dias, G. R., Coelho, A. T., Rebelo, F. and Pereira, T. (2008) 'Non-linear finite element modelling of anatomically detailed 3D foot model', *Report paper*, pp. 1–11.

Arthritis Research UK (2013) *Osteoarthritis of the knee*. Available at: https://www.arthritisresearchuk.org/.

Bendjaballah, M. Z., Shirazi-Adl, A. and Zukor, D. J. (1995) 'Biomechanics of the human knee joint in compression: reconstruction, mesh generation and finite element analysis', *The Knee*. Elsevier, 2(2), pp. 69–79. doi: 10.1016/0968-0160(95)00018-K.

Bendjaballah, M. Z., Shirazi-Adl, A. and Zukor, D. J. (1997) 'Finite element analysis of human knee joint in varus-valgus', *Clinical Biomechanics*. Elsevier, 12(3), pp. 139–148. doi: 10.1016/S0268-0033(97)00072-7.

Blankevoort, L., Kuiper, J. H., Huiskes, R. and Grootenboer, H. J. (1991) 'Articular contact in a three-dimensional model of the knee.', *Journal of biomechanics*. Elsevier, 24(11), pp. 1019–31. doi: 10.1016/0021-9290(91)90019-J.

Brilakis, E., Kaselouris, E., Xypnitos, F., Provatidis, C. G. and Efstathopoulos, N. (2012) 'Effects of Foot Posture on Fifth Metatarsal Fracture Healing: A Finite Element Study', *The Journal of Foot and Ankle Surgery*. W.B. Saunders, 51(6), pp. 720–728. doi: 10.1053/J.JFAS.2012.08.006.

Cartana, M., Tarnita, D. and Tarnita, D. (2013) 'Modelling, Simulation and Optimization of a Human Knee Orthotic Device.', *Applied Mechanics and Materials*, 371, pp. 549–553.

Cheng, H.-Y. K., Lin, C.-L., Wang, H.-W. and Chou, S.-W. (2008) 'Finite element analysis of plantar fascia under stretch—The relative contribution of windlass mechanism and Achilles tendon force', *Journal of Biomechanics*. Elsevier, 41(9), pp. 1937–1944. doi: 10.1016/J.JBIOMECH.2008.03.028.

Codamotion (2018) *3D Measurement*. Available at: https://codamotion.com/3d-measurement/ (Accessed: 1 August 2018).

Coleman, L. A. and Roubenoff, R. (2012) ‘Arthritis’, in *Encyclopedia of Human Nutrition*. doi: 10.1016/B978-0-12-375083-9.00018-0.

Darrow, M. (2001) *The Knee Sourcebook*. McGraw-Hill Education. Available at: https://books.google.co.uk/books?id=X_Eck6_o-jEC.

Derek, T., Cooke, V., Sled, E. A. and Scudamore, A. (2007) ‘Frontal plane knee alignment: a call for standardized measurement’, *The Journal of Rheumatology of Rheumatology The Journal on August*, 34(9), pp. 1796–1801. Available at: http://www.jrheum.org/content/34/9/1796.citationhttp://www.jrheum.org/alerts1.SignupforTOCsandotheralertshttp://jrheum.com/faqwww.jrheum.orgwww.jrheum.orgDownloadedfrom (Accessed: 5 August 2018).

Donahue, T. L., Hull, M. L. and Rashid, M. M. (2002) ‘A Finite Element Model of the Human Knee Joint for the Study of Tibio-Femoral Contact’, *Journal of Biomechanical Engineering*. ASME, 124(3), p. 273. doi: 10.1115/1.1470171.

Donaldson, J., Joyner, J. and Tudor, F. (2015) ‘Current Controversies of Alignment in Total Knee Replacements.’, *The open orthopaedics journal*, 9(Suppl 2: M6), pp. 489–94. doi: 10.2174/1874325001509010489.

Ethier, C. R. and Simmons, C. A. (2008) *Introductory Biomechanics from Cells to Organisms*. Cambridge University Press (Cambridge texts in biomedical engineering). Available at: https://books.google.co.uk/books?id=Dh0OuAEACAAJ.

Felson, D. T. (2006) ‘Osteoarthritis of the Knee’, *New England Journal of Medicine*. Massachusetts Medical Society , 354(8), pp. 841–848. doi: 10.1056/NEJMcp051726.

Fernandes, D. J. C. (2014) *Finite Element Analysis of the ACL-deficient Knee*.

Flavin, R., Halpin, T., O'Sullivan, R., FitzPatrick, D., Ivankovic, A. and Stephens, M. M. (2008) 'A finite-element analysis study of the metatarsophalangeal joint of the hallux rigidus', *The Journal of Bone and Joint Surgery. British volume*. The British Editorial Society of Bone & Joint Surgery, 90–B(10), pp. 1334–1340. doi: 10.1302/0301-620X.90B10.20506.

Fontanella, C. G., Matteoli, S., Carniel, E. L., Wilhjelm, J. E., Virga, A., Corvi, A. and Natali, A. N. (2012) 'Investigation on the load-displacement curves of a human healthy heel pad: In vivo compression data compared to numerical results', *Medical Engineering and Physics*. Elsevier, 34(9), pp. 1253–1259. doi: 10.1016/j.medengphy.2011.12.013.

Fosco, M., Ayad, R. Ben, Fantasia, R., Dallari, D. and Tigani, D. (2012) 'Concepts in Computer Assisted Total Knee Replacement Surgery', in *Recent Advances in Hip and Knee Arthroplasty*. InTech.

Gardiner, J. C. and Weiss, J. A. (2006) 'Subject-specific finite element analysis of the human medial collateral ligament during valgus knee loading', *Journal of Orthopaedic Research*. John Wiley & Sons, Ltd, 21(6), pp. 1098–1106. doi: 10.1016/S0736-0266(03)00113-X.

Giorgiafiorio (2018) *Human knee anatomy*. Available at: https://giorgiafiorio.org/anatomy-of-the-knee/front-view-of-knee-joint-anatomy-3/.

Grimes, B. (2018) 'A Clinical Gait Analysis Study of the Knee Joint with and without a Knee Orthotic'.

Hall, S. J. (2015) *Basic Biomechanics*. McGraw-Hill Education. Available at: https://books.google.co.uk/books?id=aH8gnwEACAAJ.

Hayes, W. C. and Mockros, L. F. (1971) 'Viscoelastic properties of human articular cartilage.', *Journal of Applied Physiology*. American Physiological Society, 31(4), pp. 562–568. doi: 10.1152/jappl.1971.31.4.562.

Hopkins, A. R., New, A. M., Rodriguez-y-Baena, F. and Taylor, M. (2010) 'Finite element analysis of unicompartmental knee arthroplasty', *Medical Engineering & Physics*. Elsevier, 32(1), pp. 14–21. doi: 10.1016/j.medengphy.2009.10.002.

Jin, Z. (2014) *Computational modelling of biomechanics and biotribology in the musculoskeletal system*. Elsevier.

John, D., Pinisetty, D. and Gupta, N. (2013) 'Image Based Model Development and Analysis of the Human Knee Joint', in Andreaus, U. and Iacoviello, D. (eds) *Biomedical Imaging and Computational Modeling in Biomechanics*. Dordrecht: Springer Netherlands, pp. 55–79. doi: 10.1007/978-94-007-4270-3_4.

Kamath, A. F., Israelite, C., Horneff, J. and Lotke, P. A. (2010) 'Editorial: What is varus or valgus knee alignment?: a call for a uniform radiographic classification.', *Clinical orthopaedics and related research*. Association of Bone and Joint Surgeons, 468(6), pp. 1702–4. doi: 10.1007/s11999-010-1334-4.

Kiapour, A., Kiapour, A. M., Kaul, V., Quatman, C. E., Wordeman, S. C., Hewett, T. E., Demetropoulos, C. K. and Goel, V. K. (2014) 'Finite Element Model of the Knee for Investigation of Injury Mechanisms: Development and Validation', *Journal of Biomechanical Engineering*. American Society of Mechanical Engineers, 136(1), pp. 110021–1100214. doi: 10.1115/1.4025692.

Kiss, R. M., Kocsis, L. and Knoll, Z. (2004) ‘Joint kinematics and spatial–temporal parameters of gait measured by an ultrasound-based system’, *Medical Engineering & Physics*. Elsevier, 26(7), pp. 611–620. doi: 10.1016/J.MEDENGPHY.2004.04.002.

Kobayashi, K., Gransberg, L., Knutsson, E. and Nolén, P. (1997) ‘A new system for three-dimensional gait recording using electromagnetic tracking’, *Gait & Posture*. Elsevier, 6(1), pp. 63–75. doi: 10.1016/S0966-6362(96)01102-2.

Levangie, P. K. and Norkin, C. C. (2011a) *Joint Structure and Function: A Comprehensive Analysis*. F.A. Davis Company (Joint Structure and Function). Available at: https://books.google.co.uk/books?id=JXb2AAAAQBAJ.

Levangie, P. K. and Norkin, C. C. (2011b) ‘The Knee’, in *Joint Structure and Function: A Comprehensive Analysis*. F.A. Davis Company (Joint Structure and Function), pp. 395–435. Available at: https://books.google.co.uk/books?id=JXb2AAAAQBAJ.

Limbert, G., Taylor, M. and Middleton, J. (2004) ‘Three-dimensional finite element modelling of the human ACL: Simulation of passive knee flexion with a stressed and stress-free ACL’, *Journal of Biomechanics*. Elsevier, 37(11), pp. 1723–1731. doi: 10.1016/j.jbiomech.2004.01.030.

Liu, T., Inoue, Y. and Shibata, K. (2010) ‘A Wearable Ground Reaction Force Sensor System and Its Application to the Measurement of Extrinsic Gait Variability’, *Sensors (Basel, Switzerland)*. Molecular Diversity Preservation International (MDPI), 10(11), pp. 10240–10255. doi: 10.3390/s101110240.

Marieb, E. N., Wilhelm, P. B., Katja Hoehn, M. D. P. D., Hutchinson, M. and

Mallatt, J. (2013) *Human Anatomy & Physiology*. Benjamin-Cummings Publishing Company. Available at: https://books.google.co.uk/books?id=oRjTnQEACAAJ.

Morales-Orcajo, E., Bayod, J. and Barbosa de Las Casas, E. (2016) 'Computational Foot Modeling: Scope and Applications', *Arch Computat Methods Eng*, 23(3), pp. 389–416. Available at: https://doi.org/10.1007/s11831-015-9146-z.

Naderi-pour, A. (2010) *Femur*, *OrthopaedicsOne*. Available at: https://www.orthopaedicsone.com/display/Review/Femur.

Nigg, B. M. and Herzog, W. (2007) *Biomechanics of the Musculo-skeletal System*. Wiley. Available at: https://books.google.co.uk/books?id=hOIeAQAAIAAJ.

Pallejà, T., Teixidó, M., Tresanchez, M. and Palacín, J. (2009) 'Measuring Gait Using a Ground Laser Range Sensor', *Sensors (Basel, Switzerland)*. Molecular Diversity Preservation International (MDPI), 9(11), pp. 9133–9146. doi: 10.3390/s91109133.

Payton, C. and Bartlett, R. (2007) *Biomechanical Evaluation of Movement in Sport and Exercise: The British Association of Sport and Exercise Sciences Guide*. Taylor & Francis (BASES Sport and Exercise Science). Available at: https://books.google.co.uk/books?id=iV59AgAAQBAJ.

Peña, E., Calvo, B., Martínez, M. A. and Doblaré, M. (2006) 'A three-dimensional finite element analysis of the combined behavior of ligaments and menisci in the healthy human knee joint', *Journal of Biomechanics*. Elsevier, 39(9), pp. 1686–1701. doi: 10.1016/j.jbiomech.2005.04.030.

Peña, E., Calvo, B., Martínez, M. A., Palanca, D. and Doblaré, M. (2005) ‘Finite element analysis of the effect of meniscal tears and meniscectomies on human knee biomechanics’, *Clinical Biomechanics*. Elsevier, 20(5), pp. 498–507. doi: 10.1016/j.clinbiomech.2005.01.009.

Peña, E., Martínez, M. A., Calvo, B., Palanca, D. and Doblaré, M. (2005) ‘A finite element simulation of the effect of graft stiffness and graft tensioning in ACL reconstruction’, *Clinical Biomechanics*. Elsevier, 20(6), pp. 636–644. doi: 10.1016/J.CLINBIOMECH.2004.07.014.

Qian, Z., Ren, L. and Ren, L. (2010) ‘A Coupling Analysis of the Biomechanical Functions of Human Foot Complex during Locomotion’, *Journal of Bionic Engineering*. No longer published by Elsevier, 7, pp. S150–S157. doi: 10.1016/S1672-6529(09)60229-8.

Rayfield, E. . (2007) ‘Finite Element Analysis and Understanding the Biomechanics and Evolution of Living and Fossil Organisms’, *Annual Review of Earth and Planetary Sciences*. Annual Reviews, 35(1), pp. 541–576. doi: 10.1146/annurev.earth.35.031306.140104.

Shirazi, R. and Shirazi-Adl, A. (2009) ‘Computational biomechanics of articular cartilage of human knee joint: Effect of osteochondral defects’, *Journal of Biomechanics*. Elsevier, 42(15), pp. 2458–2465. doi: 10.1016/j.jbiomech.2009.07.022.

Siegel, L., Vandenakker-Albanese, C. and Siegel, D. (2012) ‘Anterior cruciate ligament injuries: anatomy, physiology, biomechanics, and management’, *Clinical Journal of Sport Medicine*. LWW, 22(4), pp. 349–355.

Standring, S. and Borley, N. R. (2008) *Gray's Anatomy: The Anatomical Basis of Clinical Practice*. Churchill Livingstone/Elsevier (ClinicalKey 2012). Available at: https://books.google.co.uk/books?id=kvhkPQAACAAJ.

Sun, J., Yan, S., Jiang, Y., Wong, D. W., Zhang, M., Zeng, J. and Zhang, K. (2016) 'Finite element analysis of the valgus knee joint of an obese child', *BioMedical Engineering OnLine*. London: BioMed Central, 15(Suppl 2), p. 158. doi: 10.1186/s12938-016-0253-3.

Sun, W., Starly, B., Nam, J. and Darling, A. (2005) 'Bio-CAD modeling and its applications in computer-aided tissue engineering', *CAD Computer Aided Design*. Elsevier, 37(11), pp. 1097–1114. doi: 10.1016/j.cad.2005.02.002.

Tarniţă, D., Catana, M. and Tarnita, D. N. (2014) 'Modeling and Finite Element Analysis of the Human Knee Joint Affected by Osteoarthritis', *Key Engineering Materials*. Trans Tech Publications, 601, pp. 147–150. doi: 10.4028/www.scientific.net/KEM.601.147.

Tortora, G. J. and Derrickson, B. H. (2018) *Introduction to the Human Body*. Wiley. Available at: https://books.google.co.uk/books?id=BHpUDwAAQBAJ.

Tunca, C., Pehlivan, N., Ak, N., Arnrich, B., Salur, G. and Ersoy, C. (2017) 'Inertial Sensor-Based Robust Gait Analysis in Non-Hospital Settings for Neurological Disorders', *Sensors*. Multidisciplinary Digital Publishing Institute, 17(4), p. 825. doi: 10.3390/s17040825.

Wang, Y., Fan, Y. and Zhang, M. (2014) 'Comparison of stress on knee cartilage during kneeling and standing using finite element models', *Medical Engineering & Physics*. Elsevier, 36(4), pp. 439–447. doi:

10.1016/J.MEDENGPHY.2014.01.004.

Wei, S., Andrew, D., Binil, S. and Jae, N. (2010) ‘Computer-aided tissue engineering: overview, scope and challenges’, *Biotechnology and Applied Biochemistry*. Wiley-Blackwell, 39(1), pp. 29–47. doi: 10.1042/BA20030108.

Woo, S. L.-Y., Debski, R. E., Withrow, J. D. and Janaushek, M. A. (1999) ‘Biomechanics of Knee Ligaments’, *The American Journal of Sports Medicine*. SAGE Publications Inc STM, 27(4), pp. 533–543. doi: 10.1177/03635465990270042301.

Yang, N. H., Nayeb-Hashemi, H., Canavan, P. K. and Vaziri, A. (2010) ‘Effect of frontal plane tibiofemoral angle on the stress and strain at the knee cartilage during the stance phase of gait’, *Journal of Orthopaedic Research*. Wiley Subscription Services, Inc., A Wiley Company, 28(12), pp. 1539–1547. doi: 10.1002/jor.21174.

Yu, J., Cheung, J. T.-M., Zhang, Y. and Leung, A. K.-L. (2008) ‘Development of a finite element model of female foot for high-heeled shoe design’, *Clinical Biomechanics*. Elsevier, 23, pp. S31–S38. doi: 10.1016/J.CLINBIOMECH.2007.09.005.

Zheng, H., Black, N. D. and Harris, N. D. (2005) ‘Position-sensing technologies for movement analysis in stroke rehabilitation’, *Medical and Biological Engineering and Computing*, 43(4), pp. 413–420. doi: 10.1007/BF02344720.

Zielinska, B. and Haut Donahue, T. L. (2006) ‘3D Finite Element Model of Meniscectomy: Changes in Joint Contact Behavior’, *Journal of Biomechanical Engineering*. American Society of Mechanical Engineers, 128(1), p. 115. doi:

10.1115/1.2132370.